Three new species of the spider genus *Naphrys* Edwards (Araneae, Salticidae) under morphology and molecular data with notes in the distribution of *Naphrys acerba* (Peckham & Peckham) from Mexico (#104276)

First revision

Guidance from your Editor

Please submit by 6 Dec 2024 for the benefit of the authors .



Structure and Criteria

Please read the 'Structure and Criteria' page for guidance.



Custom checks

Make sure you include the custom checks shown below, in your review.



Author notes

Have you read the author notes on the guidance page?



Raw data check

Review the raw data.



Image check

Check that figures and images have not been inappropriately manipulated.

If this article is published your review will be made public. You can choose whether to sign your review. If uploading a PDF please remove any identifiable information (if you want to remain anonymous).

Files

Download and review all files from the <u>materials page</u>.

- 1 Tracked changes manuscript(s)
- 1 Rebuttal letter(s)
- 22 Figure file(s)
- 3 Table file(s)
- 1 Raw data file(s)

Custom checks

DNA data checks

- Have you checked the authors <u>data deposition statement?</u>
- Can you access the deposited data?
- Has the data been deposited correctly?
- Is the deposition information noted in the manuscript?

Field study

- Have you checked the authors field study permits?
- Are the field study permits appropriate?

New species checks

- Have you checked our <u>new species policies</u>?
- Do you agree that it is a new species?
- Is it correctly described e.g. meets ICZN standard?

For assistance email peer.review@peerj.com

Structure your review

The review form is divided into 5 sections. Please consider these when composing your review:

- 1. BASIC REPORTING
- 2. EXPERIMENTAL DESIGN
- 3. VALIDITY OF THE FINDINGS
- 4. General comments
- 5. Confidential notes to the editor
- You can also annotate this PDF and upload it as part of your review

When ready submit online.

Editorial Criteria

Use these criteria points to structure your review. The full detailed editorial criteria is on your guidance page.

BASIC REPORTING

- Clear, unambiguous, professional English language used throughout.
- Intro & background to show context.
 Literature well referenced & relevant.
- Structure conforms to <u>PeerJ standards</u>, discipline norm, or improved for clarity.
- Figures are relevant, high quality, well labelled & described.
- Raw data supplied (see <u>PeerJ policy</u>).

EXPERIMENTAL DESIGN

- Original primary research within Scope of the journal.
- Research question well defined, relevant & meaningful. It is stated how the research fills an identified knowledge gap.
- Rigorous investigation performed to a high technical & ethical standard.
- Methods described with sufficient detail & information to replicate.

VALIDITY OF THE FINDINGS

- Impact and novelty is not assessed.

 Meaningful replication encouraged where rationale & benefit to literature is clearly stated.
- All underlying data have been provided; they are robust, statistically sound, & controlled.



Conclusions are well stated, linked to original research question & limited to supporting results.

Standout reviewing tips



The best reviewers use these techniques

Τ	p

Support criticisms with evidence from the text or from other sources

Give specific suggestions on how to improve the manuscript

Comment on language and grammar issues

Organize by importance of the issues, and number your points

Please provide constructive criticism, and avoid personal opinions

Comment on strengths (as well as weaknesses) of the manuscript

Example

Smith et al (J of Methodology, 2005, V3, pp 123) have shown that the analysis you use in Lines 241-250 is not the most appropriate for this situation. Please explain why you used this method.

Your introduction needs more detail. I suggest that you improve the description at lines 57-86 to provide more justification for your study (specifically, you should expand upon the knowledge gap being filled).

The English language should be improved to ensure that an international audience can clearly understand your text. Some examples where the language could be improved include lines 23, 77, 121, 128 – the current phrasing makes comprehension difficult. I suggest you have a colleague who is proficient in English and familiar with the subject matter review your manuscript, or contact a professional editing service.

- 1. Your most important issue
- 2. The next most important item
- 3. ...
- 4. The least important points

I thank you for providing the raw data, however your supplemental files need more descriptive metadata identifiers to be useful to future readers. Although your results are compelling, the data analysis should be improved in the following ways: AA, BB, CC

I commend the authors for their extensive data set, compiled over many years of detailed fieldwork. In addition, the manuscript is clearly written in professional, unambiguous language. If there is a weakness, it is in the statistical analysis (as I have noted above) which should be improved upon before Acceptance.



Three new species of the spider genus *Naphrys* Edwards (Araneae, Salticidae) under morphology and molecular data with notes in the distribution of *Naphrys acerba* (Peckham & Peckham) from Mexico

 $\textbf{Juan Maldonado-Carrizales}~^1 \text{, Alejandro Valdez-Mondrag\'on}~^2 \text{, Mar\'ia L Jim\'enez-Jim\'enez}~^2 \text{, Javier Ponce-Saavedra}~^2 \text{, Mar\'ia L Jim\'enez-Jim\'enez}~^2 \text{, Mar\'ia L Jim\'enez-Jim\'enez}~^2 \text{, Mar\'ia L Jim\'enez-Jim\'enez}~^2 \text{, Javier Ponce-Saavedra}~^2 \text{, Mar\'ia L Jim\'enez-Jim\'enez}~^2 \text{, Mar\'ia L Jim\'enez-Jim\'enez-Jim\'enez-Jim\'enez-Jim\'enez-Jim\'enez-Jim\'enez-Jim\'enez-Jim\'enez-Jim\'enez-Jim\'enez-Jim\'enez-Jim\'enez-Jimenez$

Corresponding Author: Javier Ponce-Saavedra Email address: javier.ponce@umich.mx

Herein, we describe three new species of the spider genus *Naphrys* Edwards, 2003 from Mexico: *Naphrys echeri* **sp. nov.**, *Naphrys tecoxquin* **sp. nov.**, and *Naphrys tuuca* **sp. nov.** An integrative taxonomic approach was applied, utilizing data from morphology, ultra-morphology, the mitochondrial gene COI, and distribution records. Four molecular methods for species delimitation were implemented under the corrected *p*-distance Neighbor-Joining (NJ) criteria: 1) Assemble Species by Automatic Partitioning (ASAP); 2) General Mixed Yule Coalescent (GMYC); 3) Bayesian Poisson Tree Process (bPTP); and 4) Multi-rate Poisson Tree Process (mPTP). Both morphological and molecular data supported the delimitation and recognition of the three new species. The average interspecific genetic distance (*p*-distance) within the genus *Naphrys* is 14%, while the intraspecific genetic distances (*p*-distance) is < 2% for most species. We demonstrate that the natural distribution of *Naphrys* is not restricted to the Nearctic region. Furthermore, the reported localities herein represent the first with precise locations in the country for *Naphrys acerba*. In addition, a taxonomic identification key is provided for the species in the genus.

¹ Faculty of Biology, Universidad Michoacana de San Nicolás de Hidalgo, Morelia, Michoacan, Mexico

² Arachnological Collection, Centro de Investigaciones Biológicas del Noroeste, La Paz, Baja California Sur, Mexico



- 1 Three new species of the spider genus Naphrys
- 2 Edwards (Araneae, Salticidae) under morphology and
- 3 molecular data with notes in the distribution of
- 4 Naphrys acerba (Peckham & Peckham) from Mexico

Juan Maldonado-Carrizales¹, Alejandro Valdez-Mondragón², María Luisa Jiménez-Jiménez² Javier Ponce-Saavedra¹

8 9

- 10 ¹ Faculty of Biology, Entomology Laboratory, Universidad Michoacana de San Nicolás de
- 11 Hidalgo (UMSNH), Morelia, Michoacán, Mexico
- 12 ² Arachnological Collection (CARCIB), Centro de Investigaciones Biológicas del Noroeste
- 13 (CIBNOR), La Paz, Baja California Sur, Mexico

14

- 15 Corresponding Author:
- 16 Javier Ponce-Saavedra
- 17 Edificio B4 2º piso, Gral. Francisco J. Múgica S/N, Morelia, Michoacán, 58040
- 18 Email address: javier.ponce@umich.mx



Abstract

- 21 Herein, we describe three new species of the spider genus *Naphrys* Edwards, 2003 from Mexico:
- 22 Naphrys echeri sp. nov., Naphrys tecoxquin sp. nov., and Naphrys tuuca sp. nov. An integrative
- 23 taxonomic approach was applied, utilizing data from morphology, ultra-morphology, the
- 24 mitochondrial gene COI, and distribution records. Four molecular methods for species
- 25 delimitation were implemented under the corrected *p*-distance Neighbor-Joining (NJ) criteria: 1)
- 26 Assemble Species by Automatic Partitioning (ASAP); 2) General Mixed Yule Coalescent
- 27 (GMYC); 3) Bayesian Poisson Tree Process (bPTP); and 4) Multi-rate Poisson Tree Process
- 28 (mPTP). Both morphological and molecular data supported the delimitation and recognition of
- 29 the three new species. The average interspecific genetic distance (p-distance) within the genus
- 30 Naphrys is 14%, while the intraspecific genetic distances (p-distance) is $\leq 2\%$ for most species.
- 31 We demonstrate that the natural distribution of *Naphrys* is not restricted to the Nearctic region.
- 32 Furthermore, the reported localities herein represent the first with precise locations in the country
- 33 for Naphrys acerba. In addition, a taxonomic identification key is provided for the species in the
- 34 genus.

35 36

37

38

39 40

41

42 43

44

45

46

47

48 49

50

51

52 53

54

55

56 57

58

59

Introduction

The spider family Salticidae, comprised more than 6,700 described species, represents the most diverse spider family worldwide (WSC, 2024). One of the largest groups within this family is the tribe Euophryini, containing over 1,000 species within 116 genera (Edwards, 2003; Maddison, 2015; Zhang & Maddison, 2015). Euophryine species have a global distribution, primarily found in tropical regions (Zhang & Maddison, 2015; Maddison, 2015). They exhibit a remarkable uniformity in body shape, with elongate or ant-like forms uncommon, their genitalia also share some particular characteristics: the male palp typically has a simple spiral embolus, and the epigynum has windows framed by circular folds, presumably guiding the embolus during mating (Maddison, 2015).

The taxonomy of the tribe is encumbered by common morphological convergences and reversals, despite attempts at species delimitation using both morphological and molecular data. This taxonomic confusion is further compounded by the relative simplicity of Euophryini genitalia, which exhibit limited interspecific variation and hinder even genus-level identification (Zhang & Maddison, 2015).

According to Edwards (2003), most Euophryine species in the Nearctic region are small (less than 5 mm long) with compact bodies. These species often exhibit cryptic coloration (browns or grays) and possess a moderate number of setae on their bodies. The genus *Naphrys* Edwards, 2003 is as a clear representative of this group. *Naphrys* currently includes four described species restricted to North America: *Naphrys acerba* (G. W. Peckham & E. G. Peckham, 1909), *Naphrys bufoides* (Chamberlin & Ivie, 1944), *Naphrys pulex* (Hentz, 1846), and *Naphrys xerophila* (Richman, 1981) are all found in the United States. Additionally, *N. pulex* extends into Canada, and *N. acerba* has been reported in Mexico (Richman, 1981; Edwards, 2003; WSC, 2024).



In Mexico, the distribution of *N. acerba* is reported in the northeastern region, but precise locations remain unclear (Richman, 1981). Nevertheless, diverse sources (Ibarra-Núñez, Maya-Morales & Chamé-Vázquez, 2011; Maddison, 2015; Maldonado-Carrizales & Ponce-Saavedra, 2017) mention the presence of the genus in different parts of Mexico without assigning known species. This highlights the limited taxonomic knowledge about this genus in the country.

Modern taxonomy enlists a wide variety of methods and different lines of evidence to analyze and delimit lineages, as morphological evidence alone can be extremely difficult or impossible to delimit species in some cases (Hebert et al., 2003; Carstens et al., 2013, Luo et al., 2018; Nolasco & Valdez-Mondragón, 2022; Hedin & Milne, 2023). This approach recognizes the limitations of relying solely on morphology.

DNA analysis has become a crucial tool in species delimitation due to its objectivity. Unlike morphology that can be subjective and influenced by the environment, DNA offers a standardized and quantifiable measure of evolutionary divergence (Fujita et al., 2012). Nevertheless, delineating or delimiting spider species based only on molecular data is insufficient and incorrect (Hamilton, Formanowicz & Bond, 2011).

The combined use of morphological and molecular data is becoming increasingly important for species delimitation in spiders. This approach is particularly valuable in families like Salticidae, where similar appearances and sexual characteristics make traditional classification methods challenging (Trębicki et al., 2021; Cala-Riquelme, Bustamante & Salgado, 2022; Maddison et al., 2022; Courtial et al, 2023; Kumar, Gupta & Sharma, 2024; Lin et al., 2024; Phung et al., 2024). Similar successes have been achieved in other spider groups such as Mygalomorphae (Hamilton et al., 2014; Ortiz & Francke, 2016; Candia-Ramírez & Francke 2021; Ferretti, Nicoletta & Soresi, 2024), Synspermiata (Valdez-Mondragón et al., 2019; Navarro-Rodríguez & Valdez-Mondragón 2020; Navarro-Rodríguez & Valdez-Mondragón, 2024) and Araneoidea (Hedin & Milne, 2023). The combined use of methods has resulted in robust characterizations of species boundaries.

The integrative taxonomy approach has emerged to address shortcomings of each method individually, using multiple data sources and disciplines in a complementary way to identify and delimit species or lineages. In other words, integrative taxonomy is the method that aims to delimit species, the fundamental units of biodiversity, from different and complementary perspectives (Dayrat, 2005; DeSalle, Egan & Siddall, 2005; Padial et al., 2010; Padial & de la Riva, 2010).

While integrative taxonomy has been applied in various biological groups, its use in spider research remains limited (Bond et al., 2021). This highlights the potential for further exploration of integrative taxonomy within spider systematics.

In this study, we employ integrative taxonomy to describe three new species of the genus *Naphrys*. This approach utilizes morphological characters, ultra-morphology, and molecular data analyzed using both genetic-distance and tree-based methods for species delimitation. As there is no single species concept, in this work we employ the unified species concept, which is a flexible framework that incorporates elements from various species concepts such as the biological,



ecological, evolutionary, and phylogenetic concepts, to delimit species based on their status as separately evolving metapopulation lineages (De Queiroz, 2007; Schlick-Steiner et al., 2010). We also consider the biogeographical distribution records of the new species. Finally, we provide a taxonomic identification key for the species of the genus and accurate distribution data for *N. acerba* in northeastern Mexico.

105106

Materials & Methods

107 The specimens were collected and preserved in both 96% ethanol for molecular analyses and 80% ethanol with complete field data labels for morphological studies. Type specimens are 108 deposited at two biological collections: Colección de Arácnidos e Insectos, Centro de 109 Investigaciones Biológicas del Noroeste, S.C. (CARCIB), La Paz, Baja California Sur, Mexico, 110 and Colección Aracnológica de la Facultad de Biología de la Universidad Michoacana 111 (CAFBUM), Morelia, Michoacán, Mexico. The specimens were collected under the document 112 SPARN/DGVS/074492/24, Scientific Collector Permit from the Secretaría de Medio Ambiente v 113 114 Recursos Naturales (SEMARNAT), Mexico, provided to Margarita Vargas Sandoval (Director and Head curator of the CAFBUM, Faculty of Biology, Entomology Laboratory, Universidad 115 Michoacana de San Nicolás de Hidalgo). For morphological descriptions, specimens were 116 117 observed using an Amscope SM1TZ-RL-10MA stereomicroscope. All measurements are in 118 millimeters (mm). Epigyna were dissected, manually cleaned, and temporarily cleared with clove oil following the method described by Levi (1965), after digesting the internal epigynal soft 119 tissues with KOH 10%. Left male palps were dissected and cleaned manually using hypodermic 120 needles and a small brush. Both genitalia were observed under a transmitted light microscope 121 Axiostar Plus Carl Zeiss. Habitus and genitalia photographs were obtained using separate setups, 122 123 an Amscope MU1000 camera attached to an Amscope SM1TZ-RL-10MA stereomicroscope for habitus images, and a transmitted light microscope (Axiostar Plus Carl Zeiss) for genitalia. 124 Photographs were processed with the Helicon focus v8.2.2 program and edited using Adobe 125 126 Photoshop CS6. The distribution map was created using QGIS v3.32 'Lima'. Biogeographic 127 province data (.shp) were obtained from the proposed boundaries by Morrone, Escalante & 128 Rodríguez-Tapia (2017), and Escalante, Rodríguez-Tapia & Morrone (2021). Boundary data (.shp files) were sourced from USGS (2021). Finally, the topographic base layer used was 'ESRI 129 Topo' via the subprogram XYZ Tiles in QGIS. For scanning electron microscopy (SEM), 130 morphological structures were dissected, cleaned manually, dehydrated in absolute ethanol, 131 132 critical-point dried with samdri-PVT-3B equipment, and then covered with gold:palladium in a 60:40 proportion. The structures were examined under low vacuum in a Hitachi S-3000N SEM. 133 Measurements on electron micrographs are in micrometers (µm). Morphological nomenclature 134 135 mostly follows Ramirez (2014) and Zhang & Maddison (2015), with abbreviations used in the description and figures as follows: AER, anterior eyes row; PER, posterior eyes row; ALE, 136 anterior lateral eye; AME, anterior median eye; PLE, posterior lateral eye; PME, posterior 137 median eye; **OQ**, ocular quadrangle; **S**, spermatheca; **CD**, copulatory duct; **W**, window of 138 epigynum; CO, copulatory openings; FD, fertilization duct; MS, median septum; RTA, 139



retrolateral tibial apophysis; **E**, embolus; **ED**, embolic disc; **SP**, sperm pore; **T**, tegulum; **TL**, tegular lobe; **RSDL**, retrolateral sperm duct loop; **VTA**, ventral tibial apophysis; **PED**, process on embolic disc.

143144

Taxon sampling

The molecular analyses were carried out with a total of 110 specimens, including one undescribed species of *Naphrys* and three new *Naphrys* species described herein. Because this study it is not a phylogenetic analysis, we use only one outgroup taxon to root the trees, *Corticattus latus* Zhang & Maddison, which represents the genus most closely related to *Naphrys* according with Zhang & Maddison (2015) (Table 1).

150151

152

153

154

155

156

157

158

159

160

161162

163

164

165166

167

168

169 170

171

172

173

174

175

176

177178

179

DNA extraction, amplification, and sequencing

The DNA was isolated separately from all eight legs of 13 individual specimens, using proteinase K/phenol/chloroform following the protocol by Hillis et al. (1996). Briefly, all eight legs of a single spider were incubated at 60°C for 24 hours with a digestion buffer containing 400 µL saline solution, 45 µL of 1% SDS solution, and 5µL of proteinase K. After digestion, 200 uL of Phenol and 200 uL of isoamyl chloroform was added and shaken vigorously. Afterwards, samples were centrifuged at 12,000 rpm for 10 minutes. Once finished, 400 µL of upper aqueous phase was recovered, repeating the phenol/chloroform washes once more. Once the phenol/chloroform washes were done, 200 µL of phenol was added to the mixture, shaken gently, and then centrifuged immediately at 12,000 rpm for 10 minutes. 300 µL of upper aqueous phase was recovered and 750 µL of cold (-20°C) absolute ethanol was added. The mixture was then shaken gently and incubated for 12 hours at -20°C. Once incubated, it was centrifuged at 13,000 rpm for 20 minutes, and the ethanol was decanted by inversion, avoiding losing the bottom pellet. 600 µL of cold 70% ethanol (-20°C) was then added and centrifuged at 13,000 rpm for 20 minutes, with ethanol decanting by inversion while avoiding losing the bottom pellet. Finally, drying in a vacuum centrifuge was performed at 60°C for 10 minutes. Once the vial is dry, DNA is suspended in 50 μL of distilled water and stored at -20°C. After DNA extraction, the mitochondrial gene Cytochrome Oxidase subunit 1 (COI), proposed by Folmer et al (1994). was amplified (LCO1498 and HCO2198). Amplifications were carried out in a GeneAmp PCR System 2700 thermal cycler, in a total volume of 25.9 µL: 1.66 µL Buffer (5X), 1.5 µL MgCl2 (50 mM), 1.25 μL LCOI1498 (10 μM), 1.25 μL HCOI2198 (10 μM), 0.23 μL Tag (5U/μL), $0.875 \mu L dNTP$'s (10 mM), 1 $\mu L BSA (1.25 mg/\mu L)$, 16.135 $\mu L H2O$, 2 $\mu L DNA$. The PCR was set up as follows: an initial step for 1 min 30 sec at 95 °C; 35 amplification cycles of 30 sec at 94 °C (denaturation), 30 sec at 50 °C (annealing), 45 sec at 72 °C (elongation), and final elongation of 10 min at 72 °C. PCR products were checked via gel electrophoresis to analyze length and purity on 1% agarose gels with a molecular marker of 1000 bp.

DNA extractions were carried out at the Laboratorio de Biología Acuática "J. Javier Alvarado Díaz," while PCR amplifications were carried out at the Centro Multidiciplinario de Estudios en Biotecnología (CMEB), both at the Universidad Michoacana de San Nicolás de



Hidalgo (UMSNH) in Morelia, Michoacán, Mexico. Purification and sanger sequencing in both
 directions were carried out in Psomagen, Maryland, United States.

Sequence editing and alignment

The sequences were visualized in Geneious Prime v.2023.2.1 (Geneious Prime, 2023) and then manually edited using the BioEdit v. 7.7.1 program (Hall, 1999). After saving in FASTA format (.fas), the sequences were aligned using MAFFT v. 7 (Katoh & Toh 2008) with default parameters on the MAFFT online server (https://mafft.cbrc.jp/alignment/server/).

Molecular analysis and species delimitation

Four different molecular delimitation methods were employed using the corrected *p*-distances Neighbor-Joining (NJ) as initial criteria: 1) ASAP (Assemble Species by Automatic Partitioning) (Puillandre, Brouillet & Achaz, 2021), 2) GMYC (General Mixed Yule Coalescent) (Pons et al., 2006), 3) bPTP (Bayesian Poisson Tree Process) (Zhang et al., 2013), and 4) mPTP (multi-rate Poisson tree processes) (Kapli et al., 2017).

p-distances Neighbor-Joining (NJ) criteria

MEGA v.10.0.5 (Kumar et al., 2018) was used to construct the genetic distance tree, using the following parameters: number of replicates = 1000, bootstrap support values = 1000 (significant values \geq 50%), substitution type = nucleotide, model = p-distance, substitutions to include = d: transitions + transversions, rates among sites = gamma distributed with invariant sites (G+I), missing data treatment = pairwise deletion.

Assemble Species by Automatic Partitioning (ASAP)

This method is an ascending hierarchical clustering algorithm that analyzes single-locus DNA barcode datasets. It iteratively merges sequences with the highest pairwise similarity into progressively larger clusters. Additionally, ASAP retains information on all potential clustering steps, resulting in a comprehensive series of partitions representing putative species groupings within the data. Subsequently, ASAP calculates a probability score for each partition based on the within-group sequence similarity compared to between-group similarity. Finally, the method identifies the partitions with the highest probability scores as the most likely species-level groupings and constructs a species partition tree reflecting the hierarchical relationships among these putative species (Puillandre, Brouillet & Achaz, 2021). ASAP analyses were run on the online platform (https://bioinfo.mnhn.fr/abi/public/asap/) using Kimura (K80) distance matrices and configured under following parameters: substitution model = p-distances, probability = 0.01, best scores = 10, fixed seed value = -1.

General Mixed Yule Coalescent (GMYC)

The GMYC method (Fujisawa & Barraclough 2013) is a statistical framework employed for species delimitation using single-locus DNA barcode data. This approach utilizes single time



220 thresholds to define species boundaries within a Maximum Likelihood context, relying on 221 ultrametric trees as input (Ortiz & Francke 2016; Nolasco & Valdez-Mondragón, 2022). Ultrametric trees were generated in this study through phylogenetic analyses performed in 222 BEAUti and BEAST v.2.7.6 software (Bouckaert et al., 2019). A Yule Process tree prior was 223 224 implemented during the analysis to account for lineage diversification patterns. Furthermore, an optimized relaxed molecular clock model was applied, incorporating the estimated evolutionary 225 model for the COI gene (GTR + I + G). To ensure robustness of the phylogenetic inference, five 226 independent BEAST analyses were executed, each running for 80 million iterations. 227 228 Convergence of these analyses was subsequently evaluated using Tracer v1.6 (Rambaut and 229 Drummond, 2003–2013), with a minimum threshold of 200 for the Effective Sample Sizes (ESS). Following this, Tree Annotator 2.6.0 (part of the BEAST package) was employed to 230 generate maximum likelihood trees representing the most likely evolutionary histories. The first 231 232 25% of each independent run was discarded as burn-in to account for potential initial biases in the MCMC chains. Finally, the GMYC method was implemented through the online platform

234 235 236

237

238

239

240

241 242

243

244

245 246

247

248

249

233

Bayesian Poisson Tree Processes (bPTP)

(https://species.h-its.org/gmyc/) (Fujisawa & Barraclough, 2013).

bTPT operates within a Bayesian framework, accounting for uncertainties in both the phylogenetic tree's branch lengths and potential species assignments. This method assumes a Poisson process for speciation events along the tree branches and incorporates branch lengths reflecting sequence divergences. Considering this information and its inherent uncertainties, bPTP estimates posterior probabilities for various candidate species partitions within the data, which represent the likelihood of each partition accurately reflecting true species boundaries (Zhang et al., 2013). In this work, Bayesian and Maximum Likelihood variants were carried out on the online platform (https://species.h-its.org/ptp/), using following options: rooted tree, MCMC = 1000000, thinning = 100, burn-in = 0.1, seed = 123. The resulting trees were edited in FigTree 1.4.4 (Rambaut, 2018). Congruence integration criteria were employed to delimit different species. This approach compares evidence across multiple methods, resulting in more robust species delimitations and better supported species hypotheses (e.g., DeSalle, Egan & Siddall, 2005; Pons et al., 2006; Navarro-Rodríguez & Valdez-Mondragón, 2020; Valdez-Mondragón, 2020; Nolasco & Valdez-Mondragón, 2022).

250 251 252

253

254

255

256

257 258

259

Multi-rate Poisson Tree Processes (mPTP)

mPTP uses a non-homogeneous Poisson process model. This approach allows for the estimation of distinct rate multipliers for individual branches within the phylogenetic tree. recognizing potential heterogeneity in evolutionary rates across lineages. ML tree estimation was used to identify branch-specific rate multipliers, and Markov chain Monte Carlo (MCMC) simulations were employed to integrate over the uncertainty associated with these estimates (Kapli et al., 2017). By identifying statistically significant shifts in diversification rates along the tree generated from our ML analysis, mPTP pinpoints potential species boundaries, specifically



taking into account lineages that have undergone evolution at disparate paces. This analysis was carried out on the online platform (http://mptp.h-its.org/).

Zoobank

The electronic version of this article in Portable Document Format (PDF) will represent a published work according to the International Commission on Zoological Nomenclature (ICZN). Hence, the new names contained in the electronic version are effectively published under that Code from the electronic edition alone. This published work and the nomenclatural acts it contains have been registered in ZooBank, the online registration system for the ICZN. The ZooBank LSIDs (Life Science Identifiers) can be resolved, and the associated information viewed through any standard web browser by appending the LSIDs to the prefix http://zoobank.org/. The LSIDs for this publication are: urn:lsid:zoobank.org:act:6CFF43A9-8C98-4027-A1DA-2838FE4D79F8; urn:lsid:zoobank.org:act:D67CCC72-E17D-450C-9193-231120527FDE; and urn:lsid:zoobank.org:act:3129A3DE-57E8-46CC-8036-86DC467EB056. The online version of this work is archived and available from the following digital repositories:

The online version of this work is archived andPeerJ, PubMed Central SCIE, and CLOCKSS.

Results

Molecular analysis of genetic distances

The corrected *p*-distances under NJ of COI recovered six putative species (Fig. 1). Genetic distance analyses recovered groups corresponding to one putative new species (with bootstrap support value below 50%), the two previously described species *N. pulex* and *N. xerophila* (with high bootstrap support value, 89%), and three new species described herein (with high bootstrap support value, 98%). Bootstrap support values for all species were high (>89%) (Fig. 1). The average genetic *p*-interspecific distances of *Naphrys* species was 14% (min: 11%, max: 18.1%) (Table 2). Average interspecific *p*-distance between previously known species (*N. pulex* and *N. xerophila*) was 11.8%. Between new species (*N. echeri* sp. nov., *N. tecoxquin* sp. nov., and *N. tuuca* sp. nov.) and previously known species, higher interspecific average *p*-distances were observed, between 12.9% and 14%. With average values above 15.1%, *Naphrys* sp. had the highest average interspecific *p*-distance. For most species, intraspecific distances were below 1.61%, except for *Naphrys* sp. that showed a higher value (Table 3).

Molecular methods for species delimitation

The ASAP delimitation analysis recovered all six species (*N. echeri* **sp. nov.**, *N. tecoxquin* **sp. nov.**, *N. tuuca* **sp. nov.**, *Naphrys* sp., *Naphrys* pulex, and *Naphrys* xerophila) with high (>93%) bootstrap support value (Fig. 2) from the NJ tree. GMYC and mPTP methods recovered the three new species described herein and one putative new species, while *N. pulex* was not recovered as one species (Fig. 2). The most incongruent result was observed in bPTP, which delimited 42 and 50 putative species under ML and IB variants, respectively. Only *N. tecoxquin* **sp. nov.** and *N. xerophila* were recovered by the ML variant of bPTP.

PeerJ

300	Only N. xerophila was recovered under all methods and supported by a high bootstrap
301	value (93%). Naphrys pulex shows the most incongruent results in all species delimitation
302	methods, recovering 10 species in mPTP, 16 in GMYC, and 42 and 50 species in the ML and BI
303	variants of bPTP method, respectively (Fig. 2). Nevertheless, N. pulex presents low intraspecific
304	genetic distance (< 2%) and high bootstrap support value (100%) (Table 3; Fig. 2).
305	
306	Taxonomy
307	Family: Salticidae Blackwall, 1841
308	Genus: Naphrys Edwards, 2003
309	Tribe: Euophryini Simon, 1901
310	Type species: Habrocestum acerbum (G. W. Peckham & E. G. Peckham, 1909), by original
311	designation.
312	
313	Emended diagnosis. After Richman (1981) and Edwards (2003). Naphrys species are
314	characterized by their small size (2-6.1 mm) and dull, cryptic coloration (black and brown)
315	(Figs. 3C-D). Chelicera with one bicuspid promarginal tooth. Carapace high. First tibia has no
316	more than two pairs of ventral macrosetae and leg III longer than leg IV (Tibia+Patella III >
317	Tibia+Patella IV). Male palpal bulb is usually large with a proximal TL. Simple finger-like RTA
318	and RSDL present. Also, palpal tibia with ventral apophysis (VTA). Embolar disk (ED) has a
319	ventral conical projection. Embolus (E) possesses a J-shaped configuration, featuring a prolateral
320	curvature in its distal part and an emerging projection in its proximal part (Figs. 4C-H).
321	Epigynum has a typical window structure with a median septum (Figs. 5C-F). Copulatory
322	openings (CO) are positioned along posterior, median (Figs. 5C-F), or anteromedian edges of
323	atria, with atrial rims intersecting them posteriorly. Rims fail to completely encircle the atria.
324	Spermathecas (S) are nearly spherical, more or less contiguous medially, and half or more the
325	diameter of the atria. They are positioned about halfway to entirely within the posterior part of
326	atria as seen in ventral view (Figs. 5C-F).
327	
328	Current composition. Naphrys is composed of seven species: Naphrys acerba (Peckham &
329	Peckham, 1909); Naphrys bufoides (Chamberlin & Ivie, 1944); Naphrys echeri sp. nov.;
330	Naphrys pulex (Hentz, 1846); Naphrys tecoxquin sp. nov.; Naphrys tuuca sp. nov.; Naphrys
331	xerophila (Richman, 1981).
332	
333	Distribution . Canada, Mexico, and the United States.
334	
335	Remarks. We emend the generic diagnosis based on copulatory organs of male and females.
336	
337	Key to Naphrys species
338	1. Male
339	Female 8



340 341	2. Dorsum of opisthosoma with two round, bright white spots (Fig. 4A)
342 343	3. Embolus thin and straight, larger than ED (Richman 1981; Fig. 5). White setae covering all lateral side of prosoma (Edwards and Hill 2008; Fig. 7)
344	
345	Embolus thick and curve, shorter than ED (Richman 1981; Figs. 8, 16)
346	4
347 348 349	4. Dorsum of the opisthosoma with a medial longitudinal white stripe that covers the anterior portion. Anterior part of prosoma exhibits bright, coppery bronze setae across surface (Metzner 2024; Fig. 293)
350 351	Dorsum of the opisthosoma without medial longitudinal white stripe. Anterior part of prosoma is densely covered with a mixture of white, bronze, and black setae (Fig. 4A)
352	
353	5. Dorsum of opisthosoma with an extended medial white longitudinal band that extends across
354	the entire opisthosoma
355	Dorsum of opisthosoma otherwise
356	6. Embolar disk (ED) bears a well-developed triangular process, next to the embolus, clearly
357	visible in retrolateral view and smaller than embolus. Embolus thick and shorter than ED.
358	Prosoma, in dorsal view, has white setae forming a V-shape mark, extending outwards from the
359 360	sides of the PLE towards the pedicel
361	forming a gentle curve. Prosoma, in dorsal view, has white setae forming a Y-shape mark,
362	extending outwards from the sides of the PLE
363	7. Embolus thick and curved, shorter than ED (Zhang & Maddison, 2015; Fig. 140). Anterior
364	part of prosoma densely covered with a mixture of white and black setae (Edwards and Hill
365	2008; Fig. 8)
366	Embolus thick and straight. Anterior part of prosoma exhibits bright, coppery-bronze setae.
367	Legs I-III dark brown color
368	8. Copulatory openings (CO) are located on the external lateral side of the S
369	Copulatory openings (CO) located in different place
370	9. Pyriform S. Light opisthosoma with four black spots in dorsal view, along with dark brown
371	upwards chevron marks in the posterior last third
372	Circular S. Dark opisthosoma covered with coppery-bronze setae across surface and exhibiting
373	mottled pattern of faint translucent markings (Fig. 6C)
374	10. Copulatory ducts (CD) open into the epigynum forming transparent windows (W), with
375 276	openings more than one-third the length of S (Figs. 5C-F)
376 377	Copulatory ducts (CD) have circular opening, less than one-third the length of S. Copulatory openings (CO) located anteriorly to S (Richman 1981; Fig. 18). Dark opisthosoma covered with
378	brown and black setae across surface, with a longitudinal white stripe in the middle of the first



379	third and a black chevron pattern on the remaining two-thirds (Metzner 2024; Fig. 294)
380	N. xerophila (Richman, 1981)
381 382	11. Dorsum of opisthosoma with two round, bright white spots (Figs. 3C, D, 5A)
383	12 Copulatory openings (CO) located in center of epigynum, touching the anterior edge of S.
384	Copulatory ducts (CD) have a unique loop, resembling a G-shape (Figs. 5C, E)
385	
386	Copulatory openings (CO) not touching anterior edge of S (Richman 1981; Fig. 22)
387	
388	13. Copulatory openings (CO) located in the middle of epigynum (Richman 1981; Fig. 10)
389	
390	Copulatory openings (CO) located in the middle basal part of epigynum
391	
392	11. tuncu sp. 1101.
393	Naphrys acerba (Peckham & Peckham, 1909)
394	Figs. 3–5.
395	Habrocestum acerbum Peckham & Peckham, 1909, p. 522, pl. 44, figs. 1-Ic. Holotype:
396	Holotype not assigned by author. Syntypes: several males and one female from Travis County,
397	Austin, Texas, USA, and one male from Georgia, USA. NOT EXAMINED.
398	Naphrys acerba Edwards, 2003 p. 69, figs. 5-8 (Transferred from Habrocestum)
399	
400	Other material examined. MEXICO: Nuevo León: 6 females (CAFBUM88003,
401	CAFBUM88004, CABUM84234, CAFBUM84242, CAFBUM84256, CAFBUM84257), along
402	path to cable car, Cerro de la Silla, Guadalupe municipality (lat. 25.655501, long100.254415,
403	587 m), oak forest, ground hand collecting, J. Maldonado Carrizales, F. Morales Martínez, E. G.
404	Fuentes Ortiz cols., 21/X/2023. <i>Tamaulipas</i> : 3 males (CAFBUM88005) and 3 immatures
405	(CAFBUM880040), Mr. Sabino's ranch, highway Ciudad Victoria-Tula km 28 (lat. 23.606512,
406	long. 99.229572, 1473 m), oak forest, ground hand collecting, J. Maldonado Carrizales, F.
407	Morales Martínez, E. G. Fuentes Ortiz cols., 20/X/2023.
408	
409	Emended diagnosis. After Peckham & Peckham (1909) and Richman (1981). Naphrys acerba
410	resembles N. bufoides and N. xerophila by possessing white, round spots on dorsal abdomen
411	(Figs. 3C, 4A, 5A). However, it differs from N. xerophila by lacking a medial longitudinal white
412	stripe covering anterior portion. Additionally, N. acerba can be distinguished from N. bufoides
413	by its thicker embolus, which is shorter than ED (Figs. 4C, E, F, H). In females, CO of N. acerba
414	are located centrally within the epigynum, touching anterior edge of S (Figs. 5C, E). This
415	contrasts with N. bufoides, where CO do not reach anterior edge of S, and N. tuuca, where CO
416	are positioned in middle basal part of epigynum.
417	



- 418 **Distribution.** UNITED STATES: Texas; MEXICO: Coahuila, Nuevo León, Tamaulipas
- 419 [Richman, 1981; WSC, 2024], *Jalisco*, *Michoacán* and *Nayarit* [present data].

- Natural history. According to Richman (1981), this species appears to be associated with oak
- and juniper woodlands. Specimens used in this study were collected from upper leaf litter layer
- of oak forests (*Quercus* sp.) at 1473 m in Tamaulipas, Mexico, within known range of the
- 424 species. This also included disturbed areas into Monterrey City (Figs. 3A-D).

425

- 426 Naphrys echeri sp. nov.
- 427 Figs. 6–10.
- 428 LSID: urn:lsid:zoobank.org:act:FFCFC48A-1827-4DCF-9096-DE8504E63251

429

- 430 **Type material:** Male holotype, MEXICO: *Michoacán*, Cerro El Gigante, Jesús del Monte,
- 431 Morelia (lat. 19.636605, long. -101.146877, 2192 m), oak forest (*Quercus* sp.), ground hand
- 432 collecting, J. Maldonado Carrizales, F. Morales Martínez, R. Cortés Santillán cols., 31/III/2023.
- 433 (CARCIB-AR-047). Paratypes: 1 Female (CARCIB-Ar-008), 1 male (CARCIB-Ar-0327) and 1
- female (CARCIB-Ar-0328) with same collection data as for holotype. *Jalisco*: 1 male, 1
- immature (CAFBUM84264) Piedras Bolas, Ahualulco de Mercado (lat. 20.653021, long. -
- 436 104.057697, 1907 m), oak forest (*Quercus* sp.), ground hand collecting, J. Maldonado Carrizales,
- 437 G. L. López Solís, S. Montañez Hernández, N. Ruíz Hernández cols., 8/IV/2022. 1 female
- 438 (CAFBUM88012) UMA Potrero de Mulas, San Sebastián del Oeste municipality (lat.
- 439 20.749852, long. -104.976763, 797 m) cloud forest, ground hand collecting, J. Maldonado
- 440 Carrizales, E. G. Fuentes Ortiz cols., 13/XII/2022.

441

- **Other material examined.** MEXICO: *Jalisco*: 1 female (CNAN-Ar011468) and 1 male (CNAN-
- 443 Ar011467), beginning of the path to Cerro La Bufa, San Sebastián del Oeste municipality (lat.
- 444 20.758, long. -104.8438, 1460 m), young pine forest, D. Guerrero, G. Contreras, C. Hutton, G.B.
- Edwards cols., 14/VI/2018. 3 males, 3 immatures (CNAN-Ar011464), and 1 female (CNAN-
- 446 Ar011462), Piedras Bolas, Ahualulco de Mercado municipality (lat. 20.64945, long. -104.05592,
- 1863 m), oak forest (*Quercus* sp.), D. Guerrero, G. Contreras, C. Hutton and G.B. Edwards cols.,
- 448 17/VI/2018.

449

- 450 **Etymology.** The species name "echeri" (/etf eri/ native pronunciation) is a noun in apposition
- 451 that means "land or soil" in the P'urépecha language, referring to the microhabitat where it
- inhabits. The P'urépecha state, which peaked in the 14th and 15th centuries before Spanish
- 453 arrival, is known today as Michoacán, and represents the type locality of this species.

- 455 **Diagnosis.** Naphrys echeri sp. nov. resembles N. tuuca sp. nov. by males having an extended
- 456 medial white longitudinal line on dorsal part of opisthosoma, which extends across the entire
- opisthosoma (Fig. 7A). However, *N. echeri* sp. nov. differs in possessing an ED that bears a



458 well-developed triangular process (PED) next to embolus, clearly visible in retrolateral view (Figs. 7D, G. 9B, 10A-C). Naphrys echeri sp. nov. has a thick and straight E shorter than ED 459 (Figs. 7C, E, F, H), whereas in N. pulex this is thick but curved, and in N. tuuca sp. nov. the E is 460 thin and folds at midpoint forming a gentle curve, ultimately larger than ED. Naphrys echeri sp. 461 462 **nov.** differs from *N. tecoxquin* **sp. nov.** and *N. tuuca* **sp. nov.** in morphology of its embolus apex, with N. echeri sp. nov. possessing a fine projection that abruptly narrows to a spine-like structure 463 and is oriented towards the interior of the palp (Figs. 9A-B, 10A-D). Females of N. echeri sp. 464 **nov.** share with N. tecoxquin sp. nov. the placement of CO on external lateral side of S, but 465 differ in shape; in N. echeri sp. nov., S are circular (Figs. 8C-F), while in N. tecoxquin sp. nov. 466 467 they are pyriform.

468

469 **Description.** Male holotype (CARCIB-AR-047). Total length: 2.60. Prosoma 1.57 long and 1.22 wide. Darkish brown, with white setae forming a V-shaped mark, extending outwards from 470 471 sides of PLE towards pedicel in cephalic region (Fig. 7A). Lower border covered with white seta forming a band. Ocular quadrangle (OQ) 0.30 long. Anterior eyes row (AER) 1.46 times wider 472 than PER, AER 1.10 wide, PER 0.75 wide. Sternum reddish brown, 0.65 long, 0.50 wide. 473 Labium reddish brown, as long as wide, 0.30 long, 0.30 wide. Endite 0.42 long, 0.17 wide, 474 reddish brown, whitish anteriorly and square shaped (Fig. 7B). Opisthosoma 1.03 long and 0.95 475 wide: exhibiting a longitudinal band with white setae in dorsal view, covering more than half its 476 width (Fig. 7A). Palp covered by white setae in dorsal view; in ventral view possesses a straight, 477 short, and wide E that covers up to half distal part of cymbium (Figs. 7C, F, 9A, 10A). Ventral 478 view of E with scales (Figs. 10A, C). A PED is present, easily seen in retrolateral view, 479 480 triangular with fine projection on tip that abruptly narrows forming two spine-like structure (Figs. 7D, G, 9B, 10A-C). Embolus apex and SP are oriented towards interior of palp (Figs. 9A, 481 10A-B). Embolus apex presents one fine projection that abruptly narrows to a spine-like 482 structure, while SP presents a multi-convex edge forming smooth ridges (Fig. 10D). Embolar disk 483 484 (ED) completely rough and folded in anterior portion (Figs. 9A, 10A). Tegulum (T) yellow with darkish marks and wide RSDL occupying more than half of it, easily seen in retrolateral view 485 (Figs. 7D, G). Furthermore, RSDL is divided in two, anterior loop is extremely curved forming a 486 backwards "C" that extends from the middle of the T to its retrolateral edge. Posterior loop is 487 488 curved anteriorly and straight in its most posterior part, forming a backwards "L" that does not touch retrolateral edge (Figs. 7D, G). Retrolateral tibial apophysis (RTA) wide at base, becoming 489 smaller in distal part slightly anteriorly oriented (Figs. 7D, G, 9B, D). Ventral tibial apophysis 490 (VTA) rounded with a large pit at the tip. It has faint lines running across its surface (Figs. 9A, 491 C). Reddish brown legs with black bands. Legs I-II are pale with dark intersegmental markings. 492 493 except for the joint between the metatarsus and tarsus. Legs III-IV exhibit dark intersegmental markings throughout. Leg formula 3412. Leg I 2.84 (0.90, 0.45, 0.60, 0.46, 0.42), Leg II 2.72 494 (0.92, 0.45, 0.52, 0.45, 0.38), Leg III 3.90 (1.20, 0.55, 0.82, 0.77, 0.47), Leg IV 3.80 (1.30, 0.50, 495 496 0.72, 0.82, 0.45).



- 498 Female (CARCIB-Ar-008). Paler coloration, less pronounced than that of the male. Total length: 5.10. Prosoma 2.50 long and 1.90 wide. Darkish brown, with white and orange setae 499 anteriorly (Fig. 8A). Lower border covered with white setae forming a band. Ocular quadrangle 500 (OQ) 0.60 long. Anterior eyes row (AER) 1.27 times wider than PER, AER 1.40 wide, PER 1.10 501 502 wide. Sternum reddish brown with dark marks, 1.67 long, 0.87 wide. Labium black slightly longer than wide, 0.37 long, 0.32 wide. Endite 0.25 long, 0.65 wide, reddish brown, whitish 503 anteriorly and ovoid shaped (Fig. 8B). Opisthosoma 2.60 long and 2.50 wide; covered with 504 coppery bronze setae across surface and exhibiting mottled pattern of faint translucent markings 505 (Fig. 8A). Epigynum slightly wider than long, 0.40 long, 0.34 wide. Copulatory openings (CO) 506 located on external lateral sides of S. Circular S and a unique loop in CD forms a D-shape in 507 each side of epigynum (Figs. 8C-F). Median septum (MS) and sides have a smooth, trident-508 shaped with grooves or ridges on anterior part (Fig. 10E). Windows of epigynum (W) mostly 509 smooth, but striated centrally (Fig. 10E). Reddish brown legs with black marks. Leg formula 510 511 3412. Leg I 3.72 (1.12, 0.70, 0.85, 0.65, 0.40), Leg II 3.67 (1.30, 0.62, 0.67, 0.62, 0.45), Leg III
- 513514 **Distribution.** MEXICO: *Michoacán* and *Jalisco*.
- Natural history. The specimens were collected from leaf litter in oak forest (*Quercus* sp.) and cloud forest. Adults were mainly found from March to November (Figs. 6A-C).

5.52 (1.85, 0.80, 1.25, 1.00, 0.62), Leg IV 4.40 (1.57, 0.67, 1.12, 0.52, 0.50).

- 519 Naphrys tecoxquin sp. nov.
- 520 Figs. 11–15.

512

515

518

522

529

- 521 urn:lsid:zoobank.org:act:D67CCC72-E17D-450C-9193-231120527FDE
- Type material: Male holotype, MEXICO: *Jalisco*, Boca de Tomatlán, Cabo Corrientes (lat.
 20.511861, long. -105.318, 36 m), tropical forest, ground hand collecting, J. Maldonado
- 525 Carrizales, R. Cortés Santillán, E. G. Fuentes Ortiz cols., 13/IV/2023 (CARCIB-Ar-048).
- 526 Paratypes: 1 Female (CARCIB-Ar-009), 1 male (CARCIB-Ar-0329) and 1 female (CARCIB-Ar-
- 527 0330) with same collection data as holotype; 2 males (CAFBUM84260-CAFBUM84261) and 1
- female (CAFBUM84238) with same data as holotype.
- Other material examined. MEXICO. *Jalisco*: 1 male (CAFBUM84232) and 12 immatures (CAFBUM84221), same collection data as holotype. 1 imm (CNAN-Ar011469), same collection data as paratype. 1 female (CNAN-Ar011471), Las Ánimas in same municipality as holotype (lat. 20.50002, long. -105.33869, 39m), tropical forest, ground hand collecting, G. Contreras col., 6/IX/2018.
- Etymology. The species name "tecoxquin" (/tek oʃkin/ native pronunciation) is a noun inapposition in reference to the original native group that inhabited an extensive region covering

PeerJ

the entire southern coast of Nayarit and neighboring coastal of Jalisco where type locality is found.

539 540 541

542

543

544

545

546 547

548

549

550 551

552

553

554

555

538

Diagnosis. Naphrys tecoxquin sp. nov. males possess bright, coppery bronze setae in the anterior part of the Prosoma (Figs. 11E, 12A), a light opisthosoma with four black spots in dorsal view, and upwards-pointing dark brown marks in posterior third (Fig. 12A). In contrast, N. echeri sp. **nov.** exhibits a dark opisthosoma covered with coppery bronze setae across its surface and displays a mottled pattern of faint translucent markings (Fig. 7A). Naphrys tecoxquin sp. nov. exhibits dark brown legs I-III (Fig. 11E), contrasting with the rest of species. Naphrys tecoxquin **sp. nov.** is similar to *N. xerophila*, but differs in having a thick and straight embolus (Figs. 12C-H), in contrast to the curved embolus observed in N. xerophila and N. pulex. Naphrys tecoxquin **sp. nov.** differs from *N. echeri* **sp. nov.** and *N. tuuca* **sp. nov.** in morphology of its embolus apex, which is ventrally flat and dorsally convex, oriented towards the exterior of the pedipalp. The surface of the embolus apex in N. tecoxquin sp. nov. is sinuous with small projections (Fig. 15B). Additionally, *N. tecoxquin* sp. nov. lacks PED next to embolus, a characteristic of *N*. echeri sp. nov. (Figs. 7D, G, 9B, 10A-C). In females of N. tecoxquin sp. nov., CO are located on external lateral side of S (Figs. 13C, E). Naphrys tecoxquin sp. nov. differs to N. echeri sp. nov. in S shape, which is pyriform in N. tecoxquin sp. nov. (Figs. 13C-F), but round in N. echeri sp. nov. (Figs. 8C-F).

556557558

559 560

561

562

563 564

565

566

567 568

569

570

571

572

573

574

575

576 577 **Description.** Male holotype (CARCIB-Ar-048). Total length: 2.90. Prosoma 1.74 long and 1.26 wide. Darkish brown, with white setae forming a U-shaped mark, extending outwards from sides of PLE towards pedicel, anterior part is covered by bronze setae (Fig. 12A). Lower border covered with white setae forming a band. Ocular quadrangle (OQ), 0.60 long. Anterior eye row (AER) 1.31 times wider than PER, AER 1.18 wide, PER 0.90 wide. Sternum dark with faint yellow marks, 0.62 long, 0.46 wide. Labium dark, wider than long, 0.15 long, 0.22 wide. Endite 0.27 long, 0.25 wide, reddish brown, whitish anteriorly, and square shaped (Fig. 12B). Opisthosoma 1.16 long and 0.92 wide, exhibiting two straight longitudinal bands forming a "V" that cover almost half of anterior opisthosoma. In central part, there is a black mark in shape of three triangles joined at base. Additionally, a white diamond-shaped mark is present in distal part (Fig. 12A). Palp covered by white setae in dorsal view; in ventral view, a thick and straight E covers up to half of distal part of the cymbium (Figs. 12C, F). Embolus apex and SP are oriented towards exterior of the palp (Figs. 14A, 15A). Embolus apex is ventrally flat and dorsally convex, oriented towards the exterior of pedipalp. Surface of the embolus apex is sinuous with small projections (Figs. 15A-B). Embolar disk (ED) possesses a slight fold anteriorly, with striations at center (Figs. 14A, 15A). Tegulum (T) dark with faint yellow and orange marks. RSDL wide and easily seen in retrolateral view (Figs. 12D, G). Furthermore, RSDL is divided in two, anterior loop is gently curved similar to a closed parentheses ")", extended on retrolateral edge. Adjacent, the posterior loop shares the same shape, but does not touch retrolateral edge (Figs. 12D, G). Retrolateral tibial apophysis (RTA) exhibits a densely striated surface along

578 entire length. This apophysis projects in a straight orientation, gradually attenuating distally. Notably, RTA displays a slight dorsal orientation relative to the palp (Figs. 14B, D). Ventral 579 tibial apophysis (VTA) is rounded and smooth (Figs. 14A, C). Leg I, femur, patella, tibia and 580 metatarsus are dark brown with faint reddish-brown marks. Legs II-III, femur, patella and tibia 581 582 are dark brown with faint reddish-brown marks, metatarsus amber, and tarsus yellow. Leg IV, femur, metatarsus, and tarsus yellow, patella and tibia dark brown with faint blackish-brown 583 marks. Leg formula 3412. Leg I 2.81 (0.82, 0.48, 0.62, 0.45, 0.42); leg II 2.86 (0.85, 0.47, 0.60, 584 0.52, 0.41); leg III 3.83 (1.25, 0.47, 0.77, 0.81, 0.52); leg IV 3.75 (1.27, 0.58, 0.78, 0.57, 0.52). 585

586 587

588

589

590 591

592

593

594

595

596

597

598

599 600

601 602 Female (CARCIB-Ar-009). Paler coloration, less pronounced than that of the male, particularly on the prosoma. Total length: 2.68. Prosoma 1.50 long and 1.10 wide, darkish brown, with anterior part covered with black and orange setae (Fig. 13A); lower border covered with white setae forming a band. Ocular quadrangle (OQ), 0.70 long. Anterior eyes row (AER) 1.50 times wider than PER, AER 1.08 wide, PER 0.72 wide. Sternum reddish brown with dark marks, 0.62 long, 0.46 wide. Labium black, wider than long, 0.22 long, 0.46 wide. Endite 0.28 long, 0.24 wide, reddish brown, and ovoid shaped (Fig. 13B). Opisthosoma 1.18 long and 0.92 wide; light with four black spots in dorsal view, along with dark brown upwards chevron marks in posterior last third (Fig. 13A). Epigynum longer than wide, 0.82 long, 0.46 wide. Copulatory openings (CO) are located on external lateral sides of S. Pyriform S and a unique loop in CD forms a Dshape on each side of the epigynum (Figs. 13C-F). Median septum (MS) and sides smooth, trident-shaped, with grooves on anterior edges of W (Fig. 15C). Windows of epigynum (W) longer than wide, mostly smooth, but striated at center (Fig. 15C). Reddish brown legs with black marks. Leg formula 3412. Leg I 2.25 (0.67, 0.45, 0.47, 0.37, 0.27); leg II 2.12 (0.55, 0.40, 0.50, 0.35, 0.32); leg III 3.27 (1.05, 0.45, 0.70, 0.60, 0.47); leg IV 3.10 (1.00, 0.40, 0.67, 0.65, 0.37).

603 604

Distribution. MEXICO: *Jalisco*.

605

Natural history. The specimens were collected from leaf litter in tropical dry forests with broadleaved trees. Adults were mainly found from April to July and from September to November (Fig. 11).

609

- 610 Naphrys tuuca sp. nov.
- 611 Figs. 16–22.
- 612 LSID: urn:lsid:zoobank.org:act:3129A3DE-57E8-46CC-8036-86DC467EB056

- 614 Type material: Male holotype, MEXICO: Nayarit, male from Cerro San Juan, Tepic (lat.
- 615 21.505877, long. -104.924464, 1121m), oak forest (*Quercus* sp.), ground hand collecting, J.
- 616 Maldonado Carrizales, R. Cortés Santillán col., 24/V/2023 (CARCIB-Ar-049). Paratypes: 1



617 Female (CARCIB-Ar-010), 2 males (CARCIB-Ar-0331: CAFBUM880039) and 2 females (CARCIB-Ar-0332: CAFBUM880021) with same collection data as holotype. 618 619 620 Other material examined. MEXICO. Nayarit: 2 males (CAFBUM880001; CAFBUM880002), 621 1 female (CAFBUM880075), same data as holotype. 1 male (CNAN-Ar011460), same data as holotype (CNAN-Ar011461). 3 males and 3 females (CNAN-Ar011461), Ceboruco Volcano, 622 Jala municipality (lat. 21.1149, long. -104.5014, 1916m), wet glen, D. Guerrero, G. Contreras, C. 623 Hutton, and G.B. Edwards col., 16/V/2018. 624 625 **Etymology.** The species name "tuuca" (/t uuk a/ native pronunciation) is a noun in apposition 626 that means "spider" in the Wixárika language. Wixárika people are native to the Sierra Madre 627 Occidental range in Navarit state, where the type locality is found. 628 629 630 **Diagnosis.** Prosoma in dorsal view of N. tuuca sp. nov. has a unique characteristic white setae 631 forming a Y-shaped mark, extending outwards from sides of PLE (Figs. 16C, 17A). In contrast, N. echeri sp. nov. exhibits white setae forming a V-shaped mark in this region (Fig. 7A). 632 Naphrys tuuca sp. nov. has a dark opisthosoma covered with coppery-bronze setae across 633 surface (Figs. 16C, 17A), similar to N. echeri sp. nov.; nevertheless, N. tuuca sp. nov. has a 634 distinct mottled pattern of white markings and a medial longitudinal smooth white stripe that 635 covers anterior portion of the opisthosoma (Figs. 16C, 17A). Males of N. tuuca sp. nov. possess 636 a thin embolus (Figs. 17C-H). Embolus is larger than ED and folds at midpoint, forming a gentle 637 curve (Figs. 17E, H), in contrast to thin and straight embolus observed in N. bufoides. Similar to 638 639 *Naphrys tecoxquin* **sp. nov.**, embolus apex of *N. tuuca* **sp. nov.** is curved and oriented towards the exterior of palp. Surface of embolus apex in N. tuuca sp. nov. is smooth. Additionally, N. 640 tuuca sp. nov. lacks PED, which is present in N. echeri sp. nov. Females of N. tuuca sp. nov. 641 present CO located in middle basal part of epigynum (Figs. 18C, E), differing from central 642 643 location of CO observed in N. acerba, N. bufoides and N. pulex. 644 645 **Description. Male holotype (CARCIB-Ar-049).** Total length: 2.48. Prosoma 1.42 long and 1.10 wide, dark with white setae forming a Y-shaped mark, extending outwards from sides of 646 647 PLE towards pedicel (Figs. 16C, 17A). Lower border covered with white setae forming a band. Ocular quadrangle (OQ), 0.74 long. Anterior eye row (AER) 1.53 times wider than PER, AER 648 0.98 wide, PER 0.64 wide. Sternum dark with faint amber marks, 0.72 long, 0.50 wide. Labium 649 650

1.10 wide, dark with white setae forming a Y-shaped mark, extending outwards from sides of PLE towards pedicel (Figs. 16C, 17A). Lower border covered with white setae forming a band. Ocular quadrangle (OQ), 0.74 long. Anterior eye row (AER) 1.53 times wider than PER, AER 0.98 wide, PER 0.64 wide. Sternum dark with faint amber marks, 0.72 long, 0.50 wide. Labium dark, wider than long, 0.17 long, 0.25 wide. Endite 0.35 long, 0.27 wide, amber, and square-shaped (Fig. 17B). Opisthosoma 1.06 long and 0.88 wide, exhibiting a longitudinal band with white setae in dorsal view, covering one third of width (Figs. 16C, 17A). Palp covered by white setae in dorsal view, with a thin embolus in ventral view, larger than ED, which folds at midpoint, forming a gentle curve (Figs. 17C, E, F, H, 19A, 20A). Embolus apex exhibits a lateral flattening, resulting in a dorsally convex shape; oriented outwards from the main body of the palp. Embolus apex surface with smooth contours (Figs. 20A-B). Embolar disk (ED) exhibits



688 689 690

691

695

696

- 657 unfolded anterior margin, and central region displays a higher concentration of striations (Figs. 19A, 20A). Tegulum (T) dark with faint yellow and orange marks, RSDL wide, easily seen in 658 retrolateral view (Figs. 17D, G). Furthermore, RSDL is divided in two, with anterior loop 659 extremely curved, forming a backwards "C" that extends from middle of T to its retrolateral 660 661 edge. Posterior loop is curved anteriorly and straight in its most posterior part, forming a hookedshape that does not touch retrolateral edge (Figs. 17D, G). Retrolateral tibial apophysis (RTA) 662 exhibits sparse striations along its entire length. This structure projects in a straight orientation, 663 gradually attenuating distally and displaying a slight anterior orientation (Figs. 17D, G, 19B, D). 664 Ventral tibial apophysis (VTA) presents a conical structure with a roughened surface texture and 665 a small notch distally (Figs. 19A, C). Legs I-II are pale with dark intersegmental markings. 666 except for the joint between the metatarsus and tarsus. Legs III-IV exhibit dark intersegmental 667 markings throughout (Figs. 21D, H, L, P). Leg formula 3412. Leg I 2.71 (0.78, 0.47, 0.50, 0.49, 668 0.45); leg II 2.68 (0.96, 0.45, 0.51, 0.50, 0.24); leg III 3.91 (1.26, 0.65, 0.78, 0.74, 0.47); leg IV 669 3.60 (1.10, 0.45, 0.76, 0.87, 0.49). 670
- **Female (CARCIB-r-010).** Paler coloration, less pronounced than that of the male. Total length: 672 3.64. Prosoma 1.64 long and 1.34 wide, darkish brown, anterior part covered with white and 673 orange setae (Figs. 16D, E, 18A). Lower border covered with white setae forming a band. Ocular 674 quadrangle (OO) 0.68 long. Anterior eves row AER 1.47 times wider than PER. AER 1.18 wide. 675 PER 0.80 wide. Sternum reddish brown with dark marks, 0.67 long, 0.57 wide. Labium dark 676 with faint amber marks, wider than long, 0.20 long, 0.27 wide. Endite 0.37 long, 0.25 wide, 677 reddish brown, and ovoid shaped (Fig. 18B). Opisthosoma 2.00 long and 1.80 wide, dark, 678 679 covered with coppery-bronze setae across surface, with a mottled pattern of white markings and a medial longitudinal smooth white stripe covering anterior portion (Fig. 18A). Epigynum 680 slightly wider than long, 0.30 long, 0.34 wide. Copulatory openings (CO) located in middle basal 681 part of epigynum. Circular S and a unique loop in CD form a D-shape in each side of epigynum 682 683 (Figs. 18C-F). Median septum (MS) exhibits a smooth surface texture, while anterior edges of W present grooves (Fig. 20C). Overall surface of W exhibits a slightly roughened texture. Windows 684 of epigynum (W) as long as wide (Fig. 20C). Legs vellow with dark marks, metatarsus amber, 685 and tarsus yellow. Legs III and IV yellow with dark bands near segment junctions. Leg formula 686 687 3412. Leg I 2.82 (0.88, 0.52, 0.56, 0.50, 0.36); leg II 2.86 (0.92, 0.44, 0.58, 0.58, 0.34); leg III

Distribution. MEXICO: Nayarit.

Natural history. The specimens were collected from leaf litter in oak forests (*Quercus* sp.).
 Adults were mainly found from May to September. This species was observed to prey on
 Collembola (Fig. 16D).

4.14 (1.34, 0.58, 0.82, 0.90, 0.50); leg IV 4.06 (1.30, 0.56, 0.80, 0.82, 0.58).

Discussion



Species delimitation within the family Salticidae has increasingly relied on a combination of molecular and morphological data. This trend is evident in studies that employ a phylogenetic perspective (Maddison, 2016a, 2016b; Cala-Riquelme, Bustamante & Salgado, 2022; Maddison et al., 2022). While genomic data can also be a reliable approach (Girard et al. 2021; Lin, Yang & Zhang, 2024), it typically requires greater resource investments and analysis time. In contrast, studies integrating diverse data sources for species delimitation within Salticidae remain relatively scarce.

A notable example is the work by Trębicki et al. (2021), who addressed taxonomic ambiguities within the genus *Cytaea* Keyserling, 1882 and related species. The authors attributed this taxonomic confusion to poor original diagnoses and descriptions within the genus. To resolve this issue, Trębicki et al. (2021) employed a combined approach, analyzing both the morphology of the holotype specimens and utilizing the Automatic Barcode Gap Detection (ABGD) method based on a NJ tree constructed with COI gene sequences. Their results revealed that previously recognized "similar species" were synonymous with the *Cytaea* holotype, prompting the authors to formally synonymize these taxa.

While the authors employed a distance-based delimitation method (NJ tree) to clarify the identity of ambiguous species, in our work we take a more comprehensive approach, incorporating tree-based molecular analyses. To avoid future confusion, we also present an emended diagnosis of the genus *Naphrys*. These comprehensive resources aim to facilitate accurate species and genus-level determinations.

Boperachchi et al. (2022) further exemplify the application of molecular methods for species delimitation within Salticidae. Their study aimed to clarify the species diversity within the genus *Ballus* C. L. Koch, 1850 in Sri Lanka. Three species had been previously reported for this region, described in the late 19th and early 20th centuries. To address this taxonomic uncertainty, Boperachchi et al. (2022) employed a multifaceted approach, integrating morphological data with sequence data from three genes (COI, H3, 28S). They utilized multiple species delimitation methods, including ABGD, mPTP, and Bayesian Multi-Locus Species Delimitation (BPP). Notably, all applied methods yielded congruent results, indicating that the three previously recognized *Ballus* species represented a single species with consistent morphological characteristics and no significant genetic differentiation.

Similar to our work, the authors employed multiple molecular methods to investigate species diversity within a genus containing previously described species. In our study, the mPTP method, also used by Boperachchi et al. (2022), not only confirmed the identity of the previously known species *N. xeophila*, but also supported the designation of three new species.

Finally, Phung et al. (2024) employed a combined approach for species delimitation within the genus *Phintella* Strand, 1906 and related *Phintella*-like spiders. Their approach utilized three distinct methods: one distance-based method (ASAP) and two tree-based methods (Bayesian version of GMYC and BPP). These methods were used to delineate putative new species based on available genetic data. Furthermore, the authors recognized the challenge of strong sexual dimorphism within *Phintella*. They addressed this limitation by incorporating the



 same methods to assign male-female combinations for approximately one-third of the species where such pairings were unknown. The analyses by Phung et al. (2024) resulted in the identification of 22 distinct species, with 11 potentially representing undescribed taxa. Nevertheless, it is important to note that the study did not formally establish new species through the nomenclatural act.

Concordant with our findings, Phung et al. (2024) applied various methods for species delimitation. The distance-based ASAP method yielded a lower species count similar to our results. Conversely, tree-based methods (bGMYC and BPP) led to overestimations, as we also observed. Both studies endorse the utility of the COI gene for preliminary detection of potentially undescribed species, which subsequently have to be described as performed in this work.

Similar to the challenges encountered in the previous discussed studies, the Euophryini tribe exhibits numerous taxonomic uncertainties. These difficulties often stem from poor original species descriptions, limited knowledge of sexual dimorphism (e.g., only one sex known for some species), and high morphological similarity among species. To overcome these limitations, researchers have increasingly employed a combination of multiple methods (e.g., morphological and molecular data) for species delimitation (Navarro-Rodríguez & Valdez-Mondragón, 2020; Candia-Ramírez & Francke 2021; Cala-Riquelme, Bustamante & Salgado, 2022).

Morphological characters, particularly sexual characteristics, remain indispensable for robust species diagnosis, identification, and delimitation (Valdez-Mondragón, 2020). This is due, in part, to the typically low level of intraspecific variation and high level of interspecific variation observed in spider genitalia (Eberhard, 1985; Eberhard et al., 1998), making this characteristic a valuable diagnostic tool (Valdez-Mondragón, 2013; 2020; Valdez-Mondragón & Francke, 2015). In our study, we delimited different species through morphological characters, some of which were particularly diagnostic. For instance, the presence of a clearly visible PED in *N. echeri* sp. nov. and the distinctive shape of S readily distinguished this species from its congeners.

Modern taxonomic practices increasingly emphasize the integration of multiple data sources for species validation and delimitation. This combined approach strengthens the evidence for species boundaries and provides a more comprehensive understanding of the newly described taxa. In this way, the study herein represents the first where new species are described within the Salticidae family through species delimitation methods based on molecular data (both distance and tree-based).

Compared to other genes, the use of the COI gene has proven to be an effective tool for species delimitation in spiders (Trębicki et al., 2021; Valdez-Mondragón et al., 2019; Navarro-Rodríguez & Valdez-Mondragón, 2020; Nolasco & Valdez-Mondragón, 2022; Phung et al., 2024). Naseem & Muhamman (2016) identified Salticidae in citrus orchards using the COI gene with interspecific values of nucleotide divergence between 9.96–11.91%. Yamasaki et al. (2018) found higher interspecific values of nucleotide divergence (14.1–18.2%) in their redescription of the genus *Chrysilla*, based on morphology and DNA barcoding. Those studies serve as a



reference for variation among different species. The interspecific genetic divergences found in this work were greater than 11% (mean: 14%, min: 11%, max: 18.1%), fitting within the range previously reported for Salticidae.

For many taxonomic groups, a 3% genetic divergence threshold is often used to define species boundaries (Sbordoni, 2010). However, this value can vary across animal groups and even among closely related species due to differences in evolutionary rates (Trębicki et al., 2021). Previous studies (Vink, Dupérré & McQuillan, 2011; Richardson & Gunter, 2012; Blagoev et al., 2016; Trębicki et al., 2021) have reported a broad range of intraspecific genetic divergences within the Salticidae family, ranging from less than 0.5% to 7.57%.

Our results (Table 3) fit within this established range for Salticidae, except for *Naphrys* sp., which exhibited a higher divergence value of 10.94%. Unfortunately, we were unable to examinated morphologically the specimens. Our identification of this taxon was solely based on genetic data retrieved from GenBank. To conclusively determine the diagnostic characters of this species, morphological analysis is indispensable. Of note is *Naphrys pulex*, which despite inconsistencies in some species delimitation methods, showed observed intraspecific variation less than 2%, which falls well within the expected range for species of Salticidae.

Among the methods tested in this work, ASAP recovered the lowest number of species, similar to the findings by Phung et al. (2024) with Salticidae. Guo & Kong (2022) suggested that the distance-based approach is generally superior to the tree-based approach, with the ASAP method being the most efficient. As in Phung et al. (2024), our use of GMYC, bPTP, and mPTP methods resulted in a significantly higher number of delineated species. This contrast to previous studies with other groups (Mygalomorphae and Araneomorphae) of spiders (Ortiz & Francke, 2016; Valdez-Mondragón et al., 2019; Navarro-Rodríguez & Valdez-Mondragón, 2020), in which a lower number of species were typically identified using similar methods. This discrepancy might be attributed to the limitations of GMYC and PTP methods. As discussed by Luo et al. (2018) and Guo & Kong (2022), these methods can be particularly sensitive to gene flow, which can disrupt the clear correlation between population size and divergence time, potentially leading to an overestimation of species boundaries. This overestimation issue could explain the differences found in the tree-based methods of the molecular analysis for *N. pulex*, despite the low genetic intraspecific distances observed (<2%).

Hamilton, Formanowicz & Bond (2011) emphasized the utility of geographical data in species delimitation. In our study, the different *Naphrys* species present in Mexico can be separated by their distribution. *Naphrys pulex* is widespread throughout the biogeographic Alleghany subregion corresponding to eastern Canada and the United States (Escalante, Rodríguez-Tapia & Morrone, 2021). *Naphrys xerophila* is distributed only in the southeastern coastal plains of the United States through the Austroriparian biogeographic province within the Alleghany subregion (Richman, Cutler & Hill, 2012; Escalante, Rodríguez-Tapia & Morrone, 2021). Their distribution is limited by the increased aridity in the western and southern boundaries of the Alleghany subregion (Takhtajan, 1986; Escalante, Rodríguez-Tapia & Morrone, 2021).



Prior to this study, the only known species present in Mexico was *N. acerba*, which is distributed in the northern part of the Sierra Madre Oriental biogeographical province in the northeast of the country. *Naphrys tecoxquin* **sp. nov.** inhabits a distinct biogeographical province, the Pacific Lowlands. This province corresponds to a narrow, uninterrupted strip along the Pacific coast (Morrone, 2019). *Naphrys tuuca* **sp. nov.** and *N. echeri* **sp. nov.** are distributed within the Trans-Mexican Volcanic Belt (TVB) province. This province corresponds to the set of volcano mountain ranges that traverses the country from west to east (Morrone, 2019).

Within the TVB, *N. tuuca* **sp. nov.** inhabits the western mountain zone. In contrast, *N. echeri* **sp. nov.** occupies the central mountains of the TVB (Fig. 22). *Naphrys echeri* **sp. nov.** also occurs in the eastern mountains of Mexico, specifically in the northern part of the Sierra Madre del Sur (SMS) province, a mountain system that runs in parallel to the Pacific Ocean coast in a northwest-southeast direction. Nevertheless, its continuity is interrupted by a series of valleys, with rivers typically flowing above 1000 m (Hernández-Cerda, Azpra-Romero & Aguilar-Zamora, 2016; Morrone, 2019). The SMS and TVB provinces are both part of the Mexican Transition Zone (MTZ). The MTZ exhibits a unique combination of characteristics that distinguish it from other transition zones. Notably, it harbors a remarkable mixture of Nearctic and Neotropical taxa.

Geographical barriers play a key role in the differential distribution of *N. echeri* **sp. nov.** and *N. tuuca* **sp. nov.** The SMS mountain range breaks through a tectonic graben of volcanic plateaus, with stratovolcanoes developing along its margins such as the Ceboruco Volcano (Blanco y Correa, Pérez & Cruz-Medina, 2021). The easternmost locality for *N. tuuca* **sp. nov.** is separated from western localities of *N. echeri* **sp. nov.** (Piedras Bolas in the TVB and Potrero de Mulas in the SMS) by extensive alluvial plains (up to 25 km wide) and deep clefts formed by the Ameca River (Valdivia-Ornelas & Castillo-Aja, 2001; Blanco y Correa, Pérez & Cruz-Medina, 2021; Valero-Padilla, Rodríguez-Reynaga & Cruz-Angón, 2017).

The species described herein are the southernmost representatives of the genus. Contrary to prior assumptions by Edwards (2003) that the genus has a Nearctic distribution, our findings reveal the presence of these species in the Neotropical region, suggesting a broader geographical range. While the present work focused on western Mexico, further exploration particularly in the south is likely to yield additional undescribed species. This study also provides the first precise locality data for *N. acerba* within Mexico, previously known only from historical records.

Our study demonstrates the utility of the COI gene for robust species-level delimitation within the *Naphrys* genus. This finding is supported by the high congruence observed among most methods employed. Additionally, morphological characters, particularly the male palps and female epigynes, proved to be reliable features for the identification and diagnosis of *Naphrys* species.

Acknowledgements

The first author thanks the Consejo Nacional de Humanidades, Ciencia y Tecnología (CONHACYT) of Mexico for the scholarship (no. 790303) to carry out their PhD studies. The



857 858	first author also thanks the Programa Institucional de Doctorado en Ciencias Biológicas (PIDCB), Facultad de Biología, Universidad Michoacana de San Nicolás de Hidalgo (UMSNH),
859	for the academic training during the research, as well as to the PhD synodal committee for their
860	valuable contributions, comments, and suggestions in the realization of this work. The authors
861	appreciate the support of technician Ariel Arturo Cruz Villacorta in the operation of the Scanning
862	Electron Microscope (SEM) in the Electron Microscopy Laboratory at Centro de Investigaciones
863	Biológicas del Noroeste, S.C.
864	
865	References
866	Barrett DH, Hebert DN. 2005. Identifying spiders through DNA barcodes. Canadian Journal of
867	Zoology, 83(3): 481-491. https://doi.org/10.1139/z05-024
868	Bidegaray-Batista L, Arnedo MA. 2011. Gone with the plate: the opening of the Western
869	Mediterranean basin drove the diversification of ground-dweller spiders. BMC
870	Evolutionary Biology, 11(317): 1-15. https://doi.org/10.1186/1471-2148-11-317
871	Blagoev GA, deWaard JR, Ratnasingham S, deWaard L, Lu L, Robertson J, Telfer AC, Hebert
872	DN. 2016. Untangling taxonomy: A DNA barcode reference library for Canadian spiders.
873	Molecular Ecology Resources, 16: 325-341. https://doi.org/10.1111/1755-0998.12444
874	Blanco y Correa M, Pérez MAO, Cruz-Medina J. 2021. Diversidad del relieve. In: Angón AC,
875	Medina JC, Cordero, KCN, Melgarejo ED, Fong JAS, Uribe EYF, ed. La biodiversidad en
876	Nayarit. Estudio de Estado. Vol. I. México: CONABIO, 40-45.
877	Bond JE, Godwin RL, Colby JD, Newton LG, Zahnle XJ, Agnarsson I, Hamilton CA, Kuntner M.
878	2021. Improving taxonomic practices and enhancing its extensibility—an example from
879	araneology. Diversity, 14(1): 1-15. https://doi.org/10.3390/d14010005
880	Bouckaert R, Vaughan TG, Barido-Sottani J, Duchêne S, Fourment M, Gavryushkina A, Heled J,
881	Jones G, Kühnert D, De Maio N, Matschiner M, Mendes FK, Müller NF, Ogilvie HA,
882	duPlessis L, Popinga A, Rambaut A, Rasmussen D, Siveroni I, Suchard MA, Wu CH, Xie
883	D, Zhang C, Stadler T, Drummond AJ. 2019. BEAST2.5: An advanced software platform
884	for Bayesian evolutionary analysis. PLoS Computational Biology, 15(4): e1006650.
885	https://doi.org/10.1371/journal.pcbi.1006650
886	Cala-Riquelme F, Bustamante AA, Salgado A. 2022. Morphological delimitation of the genus
887	Cobanus F.O. Pickard-Cambridge, 1900 (Araneae: Salticidae: Euophryini) with a
888	description of two new species from Colombia. Zoologischer Anzeiger, 297: 42-70.
889	https://doi.org/10.1016/j.jcz.2022.02.002



390	Candia-Ramírez D, Francke O. 2021. Another stripe on the tiger makes no difference? Unexpected
391	diversity in the widespread tiger tarantula Davus pentaloris (Araneae: Theraphosidae:
392	Theraphosinae). Zoological Journal of the Linnean Society, 192(1): 75-104.
393	https://doi.org/10.1093/zoolinnean/zlaa107
394	Carstens BC, Pelletier TA, Reid NM, Satler J. 2013. How to fail at species delimitation. Molecular
395	Ecology, 22(17): 4369-4383. https://doi.org/10.1111/mec.12413
396	Caterino MS, Recuero E. 2023. Shedding light on dark taxa in sky-island Appalachian leaf litter:
397	Assessing patterns of endemicity using large-scale, voucher-based barcoding. Insect
398	Conservation and Diversity, 17(1): 16-30. https://doi.org/10.1111/icad.12697
399	Courtial C, Privet K, Aubriot X, Picard L, Pétillon J. 2023. Description of a new species of
900	Hypaeus (Araneae: Salticidae: Salticinae: Amycini) based on integrative taxonomy.
901	Studies on Neotropical Fauna and Environment, 58(2): 439-447.
902	https://doi.org/10.1080/01650521.2022.2068223
903	Dayrat B. 2005. Towards integrative taxonomy. Biological journal of the Linnean society, 85(3):
904	407-417. https://doi.org/10.1111/j.1095-8312.2005.00503.x
905	De Queiroz K. 2007. Species concepts and species delimitation. Systematic biology, 56(6): 879-
906	886. https://doi.org/10.1080/10635150701701083
907	DeSalle R, Egan MG, Siddall M. 2005. The unholy trinity: taxonomy, species delimitation and
808	DNA barcoding. Philosophical Transactions of the Royal Society B: Biological Sciences,
909	360:1905-1916. https://doi.org/10.1098%2Frstb.2005.1722
910	deWaard JR, Ratnasingham S, Zakharov EV, Borisenko AV, Steinke D, Telfer AC, Perez KHJ,
911	Sones JE, Young MR, Levesque-Beaudin V, Sobel CN, Abrahamyan A, Bessonov K,
912	Blagoev G, deWaard SL, Ho C, Ivanova NV, Layton KKS, Lu L, Manjunath R, McKeown
913	JTA, Milton MA, Miskie R, Monkhouse N, Naik S, Nikolova N, Pentinsaari M, Prosser
914	SWJ, Radulovici AE, Steinke C, Warne CP, Hebert PDN. 2019. A reference library for
915	Canadian invertebrates with 1.5 million barcodes, voucher specimens, and DNA samples.
916	Sci Data, 6: 308. https://doi.org/10.1038%2Fs41597-019-0320-2
917	Dimitrov D, Arnedo MA, Ribera C. 2008. Colonization and diversification of the spider genus
918	Pholcus Walckenaer, 1805 (Araneae, Pholcidae) in the Macaronesian archipelagos:
919	evidence for long-term occupancy yet rapid recent speciation. Molecular phylogenetics and
920	evolution, 48(2): 596-614. https://doi.org/10.1016/j.ympev.2008.04.027



921	Dimitrov D, Hormiga G. 2021. Spider diversification through space and time. Annual Review of
922	Entomology, 66: 225-241. https://doi.org/10.1146/annurev-ento-061520-083414
923	Eberhard WG. 1985. Sexual Selection and Animal Genitalia. Cambridge: Harvard university Press.
924	https://doi.org/10.4159/harvard.9780674330702
925	Eberhard WG, Huber BA, Rodriguez RL, Briceno RD, Salas I, Rodriguez V. 1998. One size fits
926	all? Relationships between the size and degree of variation in genitalia and other body parts
927	in twenty species of insects and spiders. Evolution, 52: 415-431.
928	https://doi.org/10.1111/j.1558-5646.1998.tb01642.x
929	Eberle J, Dimitrov D, Valdez-Mondragón A, Huber BA. 2018. Microhabitat change drives
930	diversification in pholcid spiders. BMC Evolutionary Biology, 18: 1-13.
931	https://doi.org/10.1186/s12862-018-1244-8
932	Edwards GB, Hill DE. 2008. Representatives of the North American salticid fauna, revisited.
933	Peckhamia, 30.2: 1-15.
934	Edwards GB. 2003. A review of the Nearctic jumping spiders (Araneae: Salticidae) of the
935	subfamily Euophryinae north of Mexico. Insecta Mundi, 16(2002): 65-75.
936	Escalante T, Rodríguez-Tapia G, Morrone JJ. 2021. Toward a biogeographic regionalization of
937	the Nearctic region: Area nomenclature and digital map. Zootaxa, 5027(3): 351-375.
938	https://doi.org/10.11646/zootaxa.5027.3.3
939	Ferretti N, Nicoletta M, Soresi DS. 2024. An integrative taxonomy approach evaluates the limits
940	of the widespread tarantula Plesiopelma longisternale (Araneae: Mygalomorphae:
941	Theraphosidae) and reveals a new species from Argentina. Zoologischer Anzeiger, 308:
942	131-143. https://doi.org/10.1016/j.jcz.2023.12.003
943	Folmer M, Black W, Lutz R, Vrijenhoek R. 1994. DNA primers for amplification of mitochondrial
944	cytochrome c oxidase subunit I from diverse metazoan invertebrates. Molecular Marine
945	Biology and Biotechnology, 3: 294–299.
946	Fujisawa T, Barraclough TG. 2013. Delimiting species using single-locus data and the Generalized
947	Mixed Yule Coalescent approach: A revised method and evaluation on simulated data sets.
948	Systematic Biology, 62(5): 707–724. https://doi.org/10.1093/sysbio/syt033
949	Fujita MK, Leaché AD, Burbrink FT, McGuire JA, Moritz C. 2012. Coalescent-based species
950	delimitation in an integrative taxonomy. Trends in ecology & evolution, 27(9): 480-488.
951	https://doi.org/10.1016/j.tree.2012.04.012



952	Generous Prime. 2023. Generous Prime 2023.2.1. Available at https://www.generous.com
953	(accesed 10 October 2023).
954	Girard MB, Elias DO, Azevedo G, Bi K, Kasumovic MK, Waldock JM, Rosenblum EB, Hedin
955	M. 2021. Phylogenomics of peacock spiders and their kin (Salticidae: Maratus), with
956	implications for the evolution of male courtship displays. Biological Journal of the Linnean
957	Society, 132(3): 471-494. https://doi.org/10.1093/biolinnean/blaa165
958	Guo B, Kong L. 2022. Comparing the Efficiency of Single-Locus Species Delimitation Methods
959	within Trochoidea (Gastropoda: Vetigastropoda). Genes, 13: 2273.
960	https://doi.org/10.3390/genes13122273
961	Hall TA. 1999. BioEdit: a user-friendly biological sequence alignment editor and analysis program
962	for Windows 95/98/NT. [Abstract] Nucleic acids symposium series 47: 95-98.
963	Hamilton CA, Formanowicz DR, Bond JE. 2011. Species delimitation and phylogeography of
964	Aphonopelma hentzi (Araneae, Mygalomorphae, Theraphosidae): Cryptic diversity in
965	North American tarantulas. PLoS ONE, 6(10): e26207.
966	https://doi.org/10.1371/journal.pone.0026207
967	Hamilton CA, Hendrixson BE, Brewer MS, Bond JE. 2014. An evaluation of sampling effects on
968	multiple DNA barcoding methods leads to an integrative approach for delimiting species:
969	A case study of the North American tarantula genus Aphonopelma (Araneae,
970	Mygalomorphae, Theraphosidae). Molecular Phylogenetics and Evolution, 71: 79-93.
971	https://doi.org/10.1016/j.ympev.2013.11.007
972	Hebert PD, Cywinska A, Ball SL, DeWaard JR. 2003. Biological identifications through DNA
973	barcodes. Proceedings of the Royal Society of London, Series B: Biological Sciences,
974	270(1512): 313-321. https://doi.org/10.1098/rspb.2002.2218
975	Hedin M, Milne MA. 2023. New species in old mountains: integrative taxonomy reveals ten new
976	species and extensive short-range endemism in Nesticus spiders (Araneae, Nesticidae)
977	from the southern Appalachian Mountains. ZooKeys, 1145: 1-130.
978	https://doi.org/10.3897/zookeys.1145.96724
979	Hernández-Cerda ME, Azpra-Romero E, Aguilar-Zamora V. 2016. Condiciones climáticas de la
980	Sierra Madre del Sur. In: Luna-Vega I, Espinosa D, Contreras-Medina R, ed. Biodiversidad
981	de la Sierra Madre del Sur: una síntesis preliminar. México: UNAM, 91-116.



982 Ibarra-Núñez G, Maya-Morales J, Chamé-Vázquez D. 2011. Las arañas del Bosque Mesófilo de 983 Montaña de la Reserva de la Biosfera Volcán Tacaná, Chiapas, México. Revista Mexicana 984 de Biodiversidad, 82(4): 1183-1193. https://doi.org/10.22201/ib.20078706e.2011.4.736 Jackson ND, Carstens BC, Morales AE, O'Meara BC. 2017. Species delimitation with gene flow. 985 Systematic biology, 66(5): 799-812. https://doi.org/10.1093/sysbio/syw117 986 Kapli P, Lutteropp S, Zhang J, Kobert K, Pavlidis P, Stamatakis A, Flouri T. 2017. Multi-rate 987 988 Poisson tree processes for single-locus species delimitation under maximum likelihood and 989 Markov chain Monte Carlo. Bioinformatics, 33(11): 1630-1638. 990 https://doi.org/10.1093/bioinformatics/btx025 991 Katoh K, Toh H. 2008. Recent developments in the MAFFT multiple sequence alignment program. 992 **MAFFT** version **Briefings** in Bioinformatics, 7. 4(4): 286-298. https://doi.org/10.1093/bib/bbn013 993 Kumar R, Gupta BK, Sharma AK. 2024. Revisiting taxonomic problems in the genus *Myrmaplata* 994 995 Prószyński, 2016 (Araneae: Salticidae). International Journal of Entomology Research, 996 9(1): 7-14. https://dx.doi.org/10.2139/ssrn.4334501 997 Kumar S, Stecher G, Li M, Knyaz C, Tamura K. 2018. MEGA X: Molecular evolutionary genetics analysis across computing platforms. Molecular Biology and Evolution, 35(6): 1547-1549. 998 999 https://doi.org/10.1093/molbev/msy096 1000 Levi HW. 1965. Techniques for the study of spider genitalia. Psyche: A Journal of entomology, 1001 72: 152-158. https://doi.org/10.1155/1965/94978 Lin L, Yang ZY, Zhang JX. 2024. Revalidation of the jumping spider genus *Cheliceroides* Żabka, 1002 1003 1985 based on molecular and morphological data (Araneae, Salticidae). ZooKeys, 1196: 1004 243-253. https://doi.org/10.3897/zookeys.1196.117921 1005 Luo A, Ling C, Ho YM, Zhu CD. 2018. Comparison of methods for molecular species delimitation 1006 across a range of speciation scenarios. Systematic Biology, 67(5): 830-846. 1007 https://doi.org/10.1093/sysbio/syy011 1008 Maddison WP, Ruiz GRS, Ng PYC, Vishnudas EH, Sudhikumar AV. 2022. Kelawakaju gen. nov., 1009 a new Asian lineage of marpissine jumping spiders (Araneae, Salticidae, Marpissina). 1010 ZooKeys, 1130: 79-102. https://doi.org/10.3897/zookeys.1130.87730 1011 Maddison WP. 2015. A phylogenetic classification of jumping spiders (Araneae: Salticidae). 1012 Journal of Arachnology, 43(3): 231-292. https://doi.org/10.1636/arac-43-03-231-292



1013	Maddison WP. 2016a. <i>Sumakuru</i> , a deeply-diverging new genus of lyssomanine jumping spiders
1014	from Ecuador (Araneae: Salticidae). ZooKeys, 614: 87-96.
1015	http://dx.doi.org/10.3897/zookeys.614.9368
1016	Maddison WP. 2016b. Papuaneon, a new genus of jumping spiders from Papua New Guinea
1017	(Araneae: Salticidae: Neonini). Zootaxa, 4200(3): 437-443.
1018	http://dx.doi.org/10.11646/zootaxa.4200.3.9
1019	Maldonado-Carrizales J, Ponce-Saavedra J. 2017. Arañas Saltarinas (Araneae: Salticidae) en dos
1020	sitios contrastantes en grado de antropización en Morelia Michoacán, México.
1021	Entomología mexicana, 4(1), 597-603.
1022	Metzner H. 2024. Jumping spiders (Arachnida: Araneae: Salticidae) of the world. Available at
1023	https://www.jumping-spiders.com (accessed 20 March 2024).
1024	Morrone JJ, Escalante T, Rodríguez-Tapia G. 2017. Mexican biogeographic provinces: Map and
1025	shapefiles. Zootaxa, 4277(2): 277-279. https://doi.org/10.11646/zootaxa.4277.2.8
1026	Morrone JJ. 2019. Regionalización biogeográfica y evolución biótica de México: encrucijada de
1027	la biodiversidad del Nuevo Mundo. Revista Mexicana de Biodiversidad, 90: e902980.
1028	https://doi.org/10.22201/ib.20078706e.2019.90.2980
1029	Naseem S, Muhamman HT. 2016. Use of mitochondrial COI gene for the identification of family
1030	Salticidae and Lycosidae of spiders. Mitochondrial DNA Part A, 29: 96-101.
1031	http://dx.doi.org/10.1080/24701394.2016.1248428
1032	Navarro-Rodríguez CI, Valdez-Mondragón A. 2024. Violins we see, species we don't Species
1033	delimitation of the spider genus Loxosceles Heineken & Lowe (Araneae: Sicariidae) from
1034	North America using morphological and molecular evidence. Zootaxa, 5428 (4): 527-548
1035	https://doi.org/10.11646/zootaxa.5428.4.4
1036	Navarro-Rodríguez I, Valdez-Mondragón A. 2020. Description of a new species of Loxosceles
1037	Heineken & Lowe (Araneae, Sicariidae) recluse spiders from Hidalgo, Mexico, under
1038	integrative taxonomy: Morphological and DNA barcoding data (CO1+ITS2). European
1039	Journal of Taxonomy, 704: 1-30. https://doi.org/10.5852/ejt.2020.704
1040	NCBI. 2024. Bethesda (MD): National Library of Medicine (US), National Center for
1041	Biotechnology Information. Available at https://www.ncbi.nlm.nih.gov/ (accessed 29
1042	September 2024).



1043	Nolasco S, Valdez-Mondragón A. 2022. To be or not to be Integrative taxonomy and species
1044	delimitation in the daddy long-legs spiders of the genus Physocyclus (Araneae, Pholcidae
1045	using DNA barcoding and morphology. ZooKeys, 1135: 93-118
1046	https://doi.org/10.3897/zookeys.1135.94628
1047	Ortiz D, Francke O. 2016. Two DNA barcodes and morphology for multi-method species
1048	delimitation in Bonnetina tarantulas (Araneae: Theraphosidae). Molecular Phylogenetics
1049	and Evolution, 101: 176-193. https://doi.org/10.1016/j.ympev.2016.05.003
1050	Padial JM, De La Riva I. 2010. A response to recent proposals for integrative taxonomy. Biologica
1051	Journal of the Linnean Society, 101(3): 747-756. https://doi.org/10.1111/j.1095-
1052	8312.2010.01528.x
1053	Padial JM, Miralles A, De la Riva I, Vences M. 2010. The integrative future of taxonomy. Frontiers
1054	in zoology, 7: 1-14. https://doi.org/10.1186/1742-9994-7-16
1055	Phung LTH, Su YC, Yamasaki T, Li YY, Eguchi K. 2024. High species diversity of <i>Phintella</i> and
1056	Phintella-like spiders (Araneae: Salticidae) in Vietnam revealed by DNA-based species
1057	delimitation analyses. Ecology and Evolution, 14: e11144
1058	https://doi.org/10.1002/ece3.11144
1059	Pons J, Barraclough TG, Gomez-Zurita J, Cardoso A, Duran DP, Hazell S, Kamoun S, Sumlin
1060	WD, Volger AP. 2006. Sequence based species delimitation for the DNA taxonomy o
1061	undescribed insects. Systematic Biology, 55(4): 595–609
1062	https://doi.org/10.1080/10635150600852011
1063	Puillandre N, Brouillet S, Achaz G. 2021. ASAP: assemble species by automatic partitioning
1064	Molecular Ecology Resources, 21(2): 609-620. https://doi.org/10.1111/1755-0998.13281
1065	Rambaut A. 2018. FigTree v1.4.4. Available at http://tree.bio.ed.ac.uk/software/figtree/ (accesed
1066	10 October 2023).
1067	Ramírez MJ. 2014. The morphology and phylogeny of dionychan spiders (Araneae
1068	Araneomorphae). Bulletin of the American Museum of Natural History, 390: 1-374
1069	http://dx.doi.org/10.1206/821.1
1070	Ratnasingham S, Hebert PDN. 2013. A DNA-Based Registry for All Animal Species: The Barcodo
1071	Index Number (BIN) System. PLoS ONE, 8(8): e66213
1072	http://www.plosone.org/article/info%3Adoi%2F10.1371%2Fjournal.pone.0066213



1073 Richardson BJ, Gunter NL. 2012. Revision of Australian jumping spider genus Servaea Simon 1074 1887 (Aranaea: Salticidae) including use of DNA sequence data and predicted 1075 distributions. Zootaxa, 3350(1): 1-33. https://doi.org/10.11646/zootaxa.3350.1.1 1076 Richman DB, Cutler B, Hill DE. 2012. Salticidae of North America, including Mexico. 1077 Peckhamia, 95(3): 1-88. Richman DB. 1981. A revision of the genus *Habrocestum* (Araneae, Salticidae) in North America. 1078 1079 Bulletin of the American Museum of Natural History, 170: 197-206. 1080 Rosenzweig ML.1995. Species Diversity in Space and Time. UK: Cambridge University Press. 1081 https://doi.org/10.1017/CBO9780511623387 1082 Sbordoni V. 2010. Strength and Limitations of DNA Barcode under the Multidimensional Species 1083 Perspective. In: Nimis PL, Lebbe RV, ed. Tools for Identifying Biodiversity: Progress and Problems. Proceedings of the International Congress. Paris, Trieste: EUT Edizioni 1084 Università di Trieste. 1085 Schlick-Steiner BC, Steiner FM, Seifert B, Stauffer C, Christian E, Crozier RH. 2010. Integrative 1086 Taxonomy: A Multisource Approach to Exploring Biodiversity. Annual Review of 1087 1088 Entomology, 55: 421–438. https://doi.org/10.1146/annurev-ento-112408-085432 1089 Stein A, Gerstner K, Kreft H. 2014. Environmental heterogeneity as a universal driver of species 1090 richness across taxa, biomes and spatial scales. Ecology Letters, 17(7): 866-80. 1091 https://doi.org/10.1111/ele.12277 1092 Takhtajan A. 1986. Floristic regions of the world. Berkeley, University of California Press. 1093 Telfer AC, Young MR, Quinn J, Perez K, Sobel CN, Sones JE, Levesque-Beaudin V, Derbyshire 1094 R, Fernandez-Triana J, Rougerie R, Thevanayagam A, Boskovic A, Borisenko AV, Cadel 1095 A, Brown A, Pages A, Castillo AH, Nicolai A, Glenn Mockford BM, Bukowski B, Wilson 1096 B, Trojahn B, Lacroix CA, Brimblecombe C, Hay C, Ho C, Steinke C, Warne CP, Garrido 1097 Cortes C, Engelking D, Wright D, Lijtmaer DA, Gascoigne D, Hernandez Martich D, 1098 Morningstar D, Neumann D, Steinke D, Marco DeBruin DD, Dobias D, Sears E, Richard 1099 E, Damstra E, Zakharov EV, Laberge F, Collins GE, Blagoev GA, Grainge G, Ansell G, 1100 Meredith G, Hogg I, McKeown J, Topan J, Bracey J, Guenther J, Sills-Gilligan J, Addesi 1101 J, Persi J, Layton KK, D'Souza K, Dorji K, Grundy K, Nghidinwa K, Ronnenberg K, Lee 1102 KM, Xie L, Lu L, Penev L, Gonzalez M, Rosati ME, Kekkonen M, Kuzmina M, Iskandar 1103 M, Mutanen M, Fatahi M, Pentinsaari M, Bauman M, Nikolova N, Ivanova NV, Jones N,



1104	Weerasuriya N, Monkhouse N, Lavinia PD, Jannetta P, Hanisch PE, McMullin RT, Ojeda
1105	Flores R, Mouttet R, Vender R, Labbee RN, Forsyth R, Lauder R, Dickson R, Kroft R,
1106	Miller SE, MacDonald S, Panthi S, Pedersen S, Sobek-Swant S, Naik S, Lipinskaya T,
1107	Eagalle T, Decaëns T, Kosuth T, Braukmann T, Woodcock T, Roslin T, Zammit T,
1108	Campbell V, Dinca V, Peneva V, Hebert PD, deWaard JR. 2015. Biodiversity inventories
1109	in high gear: DNA barcoding facilitates a rapid biotic survey of a temperate nature reserve.
1110	Biodiversity Data Journal, 30(3):e6313. https://doi.org/10.3897/bdj.3.e6313
1111	Trębicki Ł, Patoleta BM, Dabert M, Żabka M. 2021. Redescription of type species of the genus
1112	Cytaea Keyserling, 1882 (Araneae: Salticidae)an integrative approach. The European
1113	Zoological Journal, 88(1), 933-947. https://doi.org/10.1080/24750263.2021.1961029
1114	USGS. 2021. North America Political Boundaries - Sciencebase-Catalog. Available at
1115	https://www.sciencebase.gov/catalog/item/4fb555ebe4b04cb937751db9 (accesed 16
1116	January 2024).
1117	Valdez-Mondragón A, Francke OF. 2015. Phylogeny of the spider genus Ixchela Huber, 2000
1118	(Araneae: Pholcidae) based on morphological and molecular evidence (CO1 and 16S), with
1119	a hypothesized diversification in the Pleistocene. Zoological Journal of the Linnean
1120	Society, 175: 20–58. https://doi.org/10.1111/zoj.12265
1121	Valdez-Mondragón A, Navarro-Rodríguez CI, Solís-Catalán KP, Cortez-Roldán MR, Juárez-
1122	Sánchez AR. 2019. Under an integrative taxonomic approach: The description of a new
1123	species of the genus Loxosceles (Araneae, Sicariidae) from Mexico City. ZooKeys, 892:
1124	93–133. https://doi.org/10.3897/zookeys.892.39558
1125	Valdez-Mondragón A. 2013. Taxonomic revision of the spider genus Ixchela Huber, 2000
1126	(Araneae: Pholcidae), with description of ten new species from Mexico and Central
1127	America. Zootaxa, 3608 (5): 285-327. https://doi.org/10.11646/zootaxa.3608.5.1
1128	Valdez-Mondragón A. 2020. COI mtDNA barcoding and morphology for species delimitation in
1129	the spider genus Ixchela Huber (Araneae: Pholcidae), with the description of two new
1130	species from Mexico. Zootaxa, 4747(1): 54-76. doi:10.11646/zootaxa.4747.1.2
1131	Valdivia-Ornela L, Castillo-Aja MR. 2001. Las regiones geomorfológicas del estado de Jalisco.
1132	Revista Geocalli, 2(3): 17-108.

PeerJ

1133	Valero-Padilla J, Rodríguez-Reynaga FP, Cruz-Angón A. 2017. Resumen ejecutivo. Contexto
1134	físico. In: Angón AC, Hermosillo, AO, Padilla JV, Melgarejo ED, ed. La biodiversidad en
1135	Jalisco. Estudio de Estado. Vol. I. México: CONABIO, 21-22.
1136	Vink C, Dupérré N, McQuillan BN. 2011. The black-headed jumping spider, Trite planiceps
1137	Simon, 1899 (Araneae: Salticidae): redescription including cytochrome c oxidase subunit
1138	1 and paralogous 28S sequences. New Zealand Journal of Zoology, 38(4): 317-331.
1139	http://dx.doi.org/10.1080/03014223.2011.613939
1140	WSC. 2024. World Spider Catalog. Version 24. Natural History Museum Bern. Available at
1141	http://wsc.nmbe.ch (accesed 27 April 2024). https://doi.org/10.24436/2
1142	Xu X, Liu F, Cheng R-C, Chen J, Xu X, Zhang Z, Ono H, Pham DS, Norma-Rashid Y, Arnedo
1143	MA, Kuntner M, Li D. 2015. Extant primitively segmented spiders have recently
1144	diversified from an ancient lineage. Proceedings of the Royal Society B: Biological
1145	Sciences, 282(1808): 20142486. https://doi.org/10.1098/rspb.2014.2486
1146	Yamasaki T, Yamaguchi M, Phung LTH, Huang PS, Tso IM. 2018. Redescription of Chrysilla
1147	lauta Thorell 1887 (Araneae: Salticidae) based on the comparison with the holotype, and
1148	DNA barcoding. Acta Arachnologica, 67(1): 23–29. http://dx.doi.org/10.2476/asjaa.67.23
1149	Zhang J, Kapli P, Pavlidis P, Stamatakis A. 2013. A general species delimitation method with
1150	applications to phylogenetic placements. Bioinformatics, 29(22): 2869–2876.
1151	https://doi.org/10.1093/bioinformatics/btt499
1152	Zhang J, Maddison WP. 2015. Genera of euophryine jumping spiders (Araneae: Salticidae), with
1153	a combined molecular-morphological phylogeny. Zootaxa, 3938(1): 1-147.
1154	https://doi.org/10.11646/zootaxa.3938.1.1



Table 1(on next page)

Specimens used in the molecular analyses under COI, DNA voucher numbers, localities, and GenBank/BOLD accession numbers.



1 Table 1. Specimens used in the molecular analyses under COI, DNA voucher numbers, localities, and

2 GenBank/BOLD accession numbers.

Specie	DNA voucher numbers	Locality	GenBank/BO LD accesion number	Source
Naphrys pulex	Npulex_CAN1	Canada: Ontario	HM880192	Blagoev et al (2016)
	Npulex_CAN2	Canada: Wellintong	GU682819	Blagoev et al (2016)
	Npulex_CAN3	Canada: Wellintong	GU682817	Blagoev et al (2016)
	Npulex_CAN4	Canada: Wellintong	GU682816	Blagoev et al (2016)
	Npulex_CAN5	Canada: Wellintong	GU682814	Blagoev et al (2016)
	Npulex_CAN6	Canada: Wellintong	GU682836	Blagoev et al (2016)
	Npulex_CAN7	Canada: Wellintong	ARONT843- 18	Blagoev et al (2016)
	Npulex_CAN8	Canada: Wellintong	ARONT876	Ratnasingham & Hebert (2013)
	Npulex_CAN9	Canada: Ontario	ARONT917	Ratnasingham & Hebert (2013)
	Npulex_CAN10	Canada: Wellintong	ARONT947	Ratnasingham & Hebert (2013)
	Npulex_CAN11	Canada: Ontario	KP646979	Blagoev et al (2016)
	Npulex_CAN12	Canada: Ontario	KP656563	Blagoev et al (2016)
	Npulex_CAN13	Canada: Ontario	MG049224	Ratnasingham & Hebert (2013)
	Npulex_CAN14	Canada: Ontario	ARONZ306	Ratnasingham & Hebert (2013)
	Npulex_CAN15	Canada: Ontario	ARONZ331	Ratnasingham & Hebert (2013)
	Npulex_CAN16	Canada: Ontario	ARONZ571	Ratnasingham & Hebert (2013)
	Npulex_CAN17	Canada: Ontario	HQ924681	Blagoev et al (2016)
	Npulex_CAN18	Canada: Ontario	HQ924683	Blagoev et al (2016)
	Npulex_CAN19	Canada: Nova Scotia	GU683271	Blagoev et al (2016)



Npulex_CAN20	Canada: Nova Scotia	GU683271	Blagoev et al (2016)
Npulex_CAN21	Canada: Ontario	MF816087	deWaard et al (2019)
Npulex_CAN22	Canada: Nova Scotia	KP652066	Blagoev et al (2016)
Npulex_CAN23	Canada: Quebec	KP646121	Blagoev et al (2016)
Npulex_CAN24	Canada: Ontario	MF808927	deWaard et al (2019)
Npulex_CAN25	Canada: Ontario	MF816952	deWaard et al (2019)
Npulex_CAN26	Canada: Ontario	KP651428	Blagoev et al (2016)
Npulex_CAN27	Canada: Ontario	KP648109	Blagoev et al (2016)
Npulex_CAN28	Canada: Ontario	MF810509	deWaard et al (2019)
Npulex_CAN29	Canada: Ontario	ELPCG2846	Ratnasingham & Hebert (2013)
Npulex_CAN30	Canada: Ontario	ELPCG2847	Ratnasingham & Hebert (2013)
Npulex_CAN31	Canada: Ontario	ELPCG3050	Ratnasingham & Hebert (2013)
Npulex_CAN32	Canada: Ontario	ELPCG3523	Ratnasingham & Hebert (2013)
Npulex_CAN33	Canada: Ontario	ELPCG3524	Ratnasingham & Hebert (2013)
Npulex_CAN34	Canada: Ontario	ELPCG3525	Ratnasingham & Hebert (2013)
Npulex_CAN35	Canada: Ontario	ELPCG3599	Ratnasingham & Hebert (2013)
Npulex_CAN36	Canada: Ontario	ELPCG5003	Ratnasingham & Hebert (2013)
Npulex_CAN37	Canada: Ontario	ELPCG5472	Ratnasingham & Hebert (2013)
Npulex_CAN38	Canada: Ontario	ELPCG6449	Ratnasingham & Hebert (2013)
Npulex_CAN39	Canada: Ontario	ELPCG7399	Ratnasingham & Hebert (2013)
Npulex_CAN40	Canada: Ontario	ELPCG7401	Ratnasingham & Hebert (2013)
Npulex_CAN41	Canada: Ontario	ELPCG8416	Ratnasingham &



			Hebert (2013)
Npulex_CAN42	Canada: Ontario	ELPCG8449	Ratnasingham &
			Hebert (2013)
Npulex_CAN43	Canada: Ontario	ELPCG8644	Ratnasingham &
			Hebert (2013)
Npulex_CAN44	Canada: Ontario	ELPCH2306	Ratnasingham &
			Hebert (2013)
Npulex_CAN45	Canada: Ontario	MG048013	deWaard et al
			(2019)
Npulex_CAN47	Canada: Nova Scotia	KP649884	Blagoev et al
			(2016)
Npulex_CAN48	Canada: Nova Scotia	KP654153	Blagoev et al
			(2016)
Npulex_CAN49	Canada: Ontario	KP652349	Blagoev et al
- -			(2016)
Npulex CAN50	Canada: Nova Scotia	MF809281	deWaard et al
• –			(2019)
Npulex CAN51	Canada: Nova Scotia	MF813033	deWaard et al
			(2019)
Npulex CAN52	Canada: Ontario	OPPKG2671	Ratnasingham &
			Hebert (2013)
Npulex CAN53	Canada: Ontario	OPPOG1872	Ratnasingham &
			Hebert (2013)
Npulex CAN54	Canada: Ontario	OPPZE1286	Ratnasingham &
			Hebert (2013)
Npulex_CAN55	Canada: Wellintong	KP647608	Blagoev et al
			(2016)
Npulex_CAN56	Canada: Ontario	KM839902	Blagoev et al
			(2016)
Npulex_CAN57	Canada: Ontario	JN308610	Blagoev et al
			(2016)
Npulex_CAN58	Canada: Ontario	JN308622	Blagoev et al
			(2016)
Npulex_CAN59	Canada: Ontario	JN308631	Blagoev et al
			(2016)
Npulex_CAN60	Canada: Ontario	JN308807	Blagoev et al
_			(2016)
Npulex_CAN61	Canada: Ontario	JN308822	Blagoev et al
			(2016)
Npulex_CAN62	Canada: Ontario	RARBB197	Ratnasingham &
_			Hebert (2013)
Npulex_CAN63	Canada: Ontario	RARBB202	Ratnasingham &
_			Hebert (2013)
			. , ,



Npulex_CAN64	Canada: Ontario	DQ127443	Barrett & Hebert (2005)
Npulex_CAN65	Canada: Ontario	DQ127431	Barrett & Hebert (2005)
Npulex_CAN66	Canada: Ontario	RBGBB303	Ratnasingham & Hebert (2013)
Npulex_CAN67	Canada: Ontario	ROUGE2474	Ratnasingham & Hebert (2013)
Npulex_CAN68	Canada: Ontario	KT707577	Telfer et al (2015)
Npulex_CAN69	Canada: Ontario	KT707910	Telfer et al (2015)
Npulex_CAN70	Canada: Ontario	KT706489	Telfer et al (2015)
Npulex_CAN71	Canada: Ontario	KT619474	Telfer et al (2015)
Npulex_CAN72	Canada: Ontario	MG048049	Ratnasingham & Hebert (2013)
Npulex_CAN73	Canada: Ontario	MG046695	Ratnasingham & Hebert (2013)
Npulex_CAN74	Canada: Ontario	MG044990	Ratnasingham & Hebert (2013)
Npulex_CAN75	Canada: Ontario	HQ977049	Blagoev et al (2016)
Npulex_CAN76	Canada: Ontario	KP650393	Blagoev et al (2016)
Npulex_CAN77	Canada: Ontario	KP656197	Blagoev et al (2016)
Npulex_CAN78	Canada: Ontario	KP646924	Blagoev et al (2016)
Npulex_CAN79	Canada: Ontario	KP656484	Blagoev et al (2016)
Npulex_CAN80	Canada: Ontario	KP649929	Blagoev et al (2016)
Npulex_CAN81	Canada: Ontario	MG046512	Ratnasingham & Hebert (2013)
Npulex_CAN82	Canada: Ontario	MG043132	Ratnasingham & Hebert (2013)
Npulex_CAN83	Canada: Ontario	MF815739	deWaard et al (2019)
Npulex_CAN84	Canada: Ontario	MG509225	deWaard et al (2019)
Npulex_CAN85	Canada: Ontario	MG509777	deWaard et al



				(2019)
	Npulex_CAN86	Canada: Ontario	KP656878	Blagoev et al (2016)
	Npulex_CAN87	Canada: Ontario	KP656232	Blagoev et al (2016)
	Npulex_USA2	United States: Texas	BBUSE1504 (BIOUG01877 -H01)	Ratnasingham & Hebert (2013)
	Npulex_USA3	United States: Tennessee	GMGSQ008 (BIOUG03453 -H09)	Ratnasingham & Hebert (2013)
	Npulex_USA4	United States: Tennessee	GMGST563 (BIOUG04938 -E01)	Ratnasingham & Hebert (2013)
	Npulex_USA5	United States: Washington	GMNCF099	Ratnasingham & Hebert (2013)
	Npulex_USA6	United States: Unknown	OR235169	NCBI (2024)
Naphrys xerophila	Nxerophila_USA1	United States: Texas	BBUSE1415 (BIOUG01637 -H07)	Ratnasingham & Hebert (2013)
Naphrys sp.	Nsp_USA10	United States: High Appalachian Mountains	OR174102	Caterino & Recuero (2023)
	Nsp_USA11	United States: High Appalachian Mountains	OR173350	Caterino & Recuero (2023)
	Nsp_USA8	United States: High Appalachian Mountains	OR174487	Caterino & Recuero (2023)
	Nsp_USA9	United States: High Appalachian Mountains	OR174414	Caterino & Recuero (2023)
Naphrys echeri sp. nov.	Necheri_MEX11	Mexico: Michoacán	PP123908	Present study
	Necheri_MEX58	Mexico: Michoacán	PP123905	Present study
	Necheri_MEX71	Mexico: Michoacán	PP123902	Present study
	Necheri_MEX73	Mexico: Michoacán	PP123909	Present study
	Necheri_MEX74	Mexico: Michoacán	PP123903	Present study
	Necheri_MEX8	Mexico: Michoacán	PP123900	Present study
	Necheri_MEX9	Mexico: Michoacán	PP123901	Present study
Naphrys tecoxquin	Ntecoxquin MEX1	Mexico: Jalisco	PP123899	Present study



	Ntecoxquin_MEX5	Mexico: Jalisco	PP123898	Present study
	Ntecoxquin_ MEX 56	Mexico: Jalisco	PP123906	Present study
Naphrys tuuca sp. nov.	Ntuuca_ MEX 52	Mexico: Nayarit	PP123904	Present study
	Ntuuca_ MEX 76	Mexico: Nayarit	PP123910	Present study
	Ntuuca_ MEX 98	Mexico: Nayarit	PP123907	Present study
Corticattus latus	Clatus_DomRep	Dominican Republic:	KC615698	Zhang &
		Pedernales		Maddison
				(2015)



Table 2(on next page)

Average genetic distances (p-distances) of COI among Naphrys species.



1 Table 2. Average genetic distances (p-distances) of COI among Naphrys species.

	1	2	3	4	5
1. Naphrys pulex USA	-				
2. Naphrys xerophila USA	11.8	-			
3. Naphrys sp. USA	15.1	16.4	-		
4. Naphrys tecoxquin sp. nov. MEX	14.0	12.9	18.1	-	
5. Naphrys echeri sp. nov. MEX	13.4	13.4	17.8	11.2	-
6. Naphrys tuuca sp. nov. MEX	13.0	13.6	17.2	11.0	11.1

2



Table 3(on next page)

Average genetic distance (p-distances) of COI within Naphrys species.



1 Table 3. Average genetic distance (*p*-distances) of COI within *Naphrys* species.

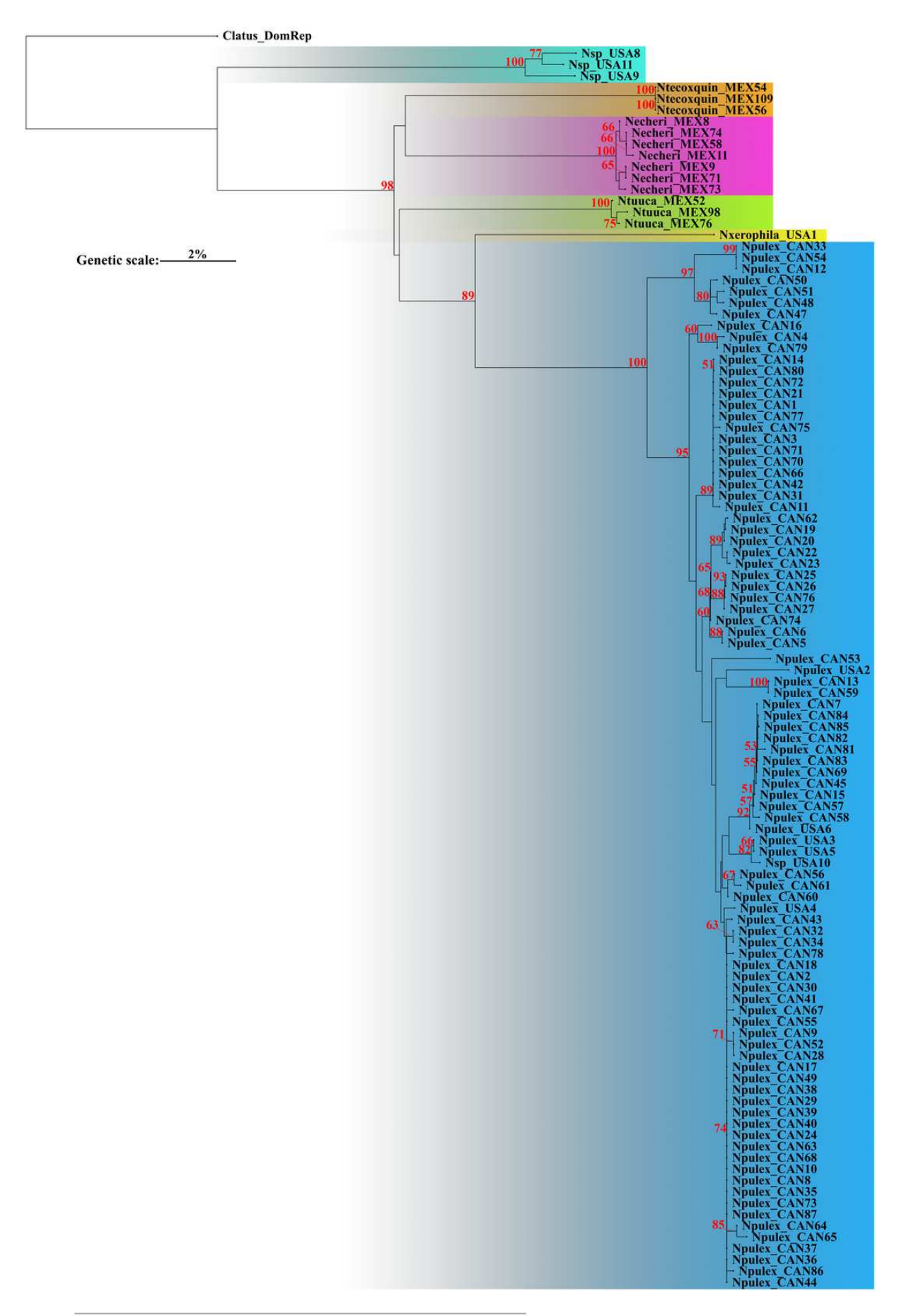
Specie	Distance	Standard
		Error
Naphrys pulex USA	1.61	0.26
Naphrys xerophila USA	-	-
Naphrys sp. USA	10.94	1.18
Naphrys tecoxquin sp. nov. MEX	0	0
Naphrys echeri sp. nov. MEX	0.32	0.15
Naphrys tuuca sp. nov. MEX	0.34	0.19



Neighbor-Joining (NJ) with corrected *p*-distances tree constructed with COI sequences from different species of *Naphrys*.

Colors indicate putative species. Red numbers above branches represent significant Bootstrap support values (> 50%).



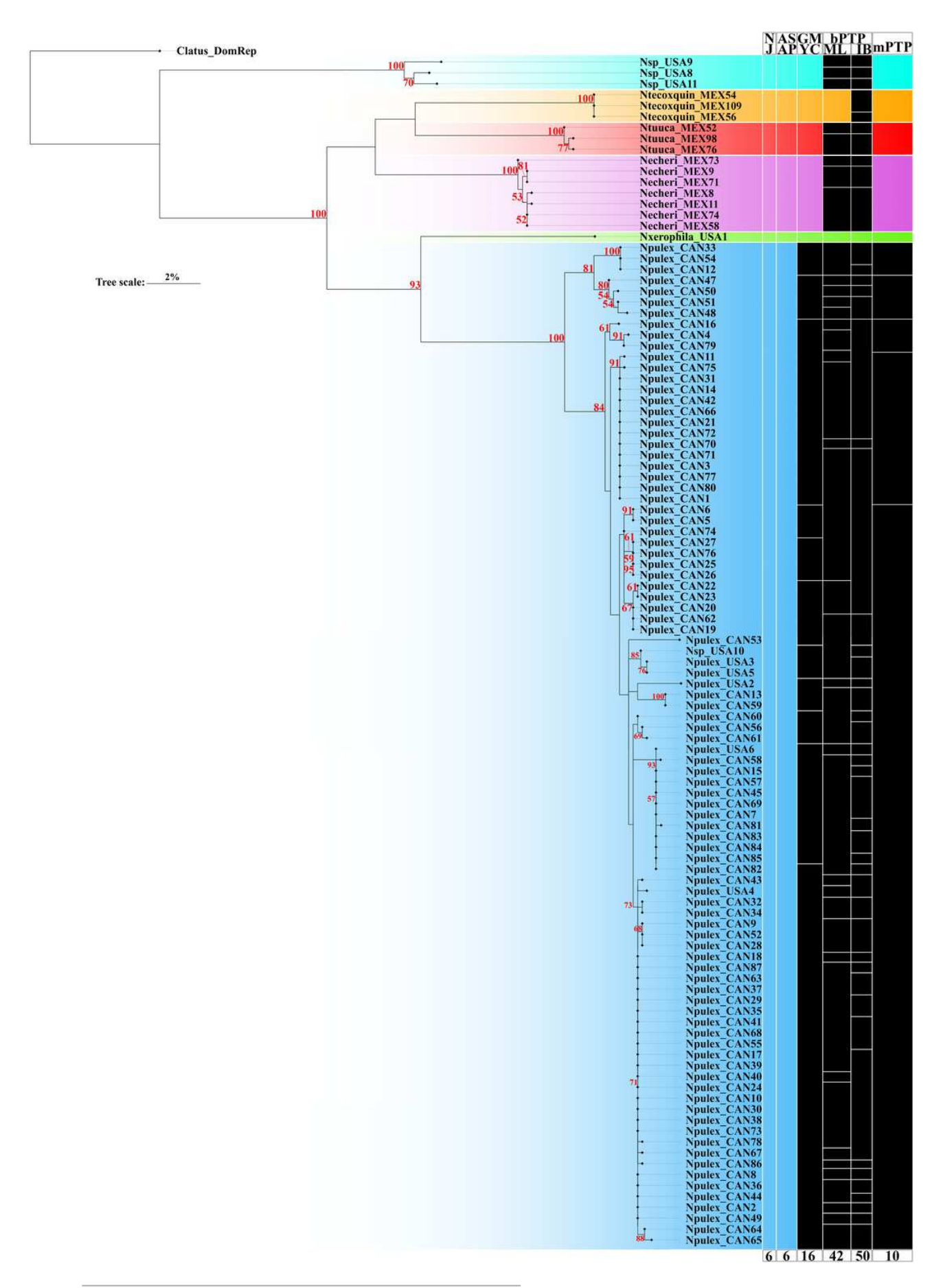




Maximum Likelihood (ML) tree of Naphrys constructed with COI.

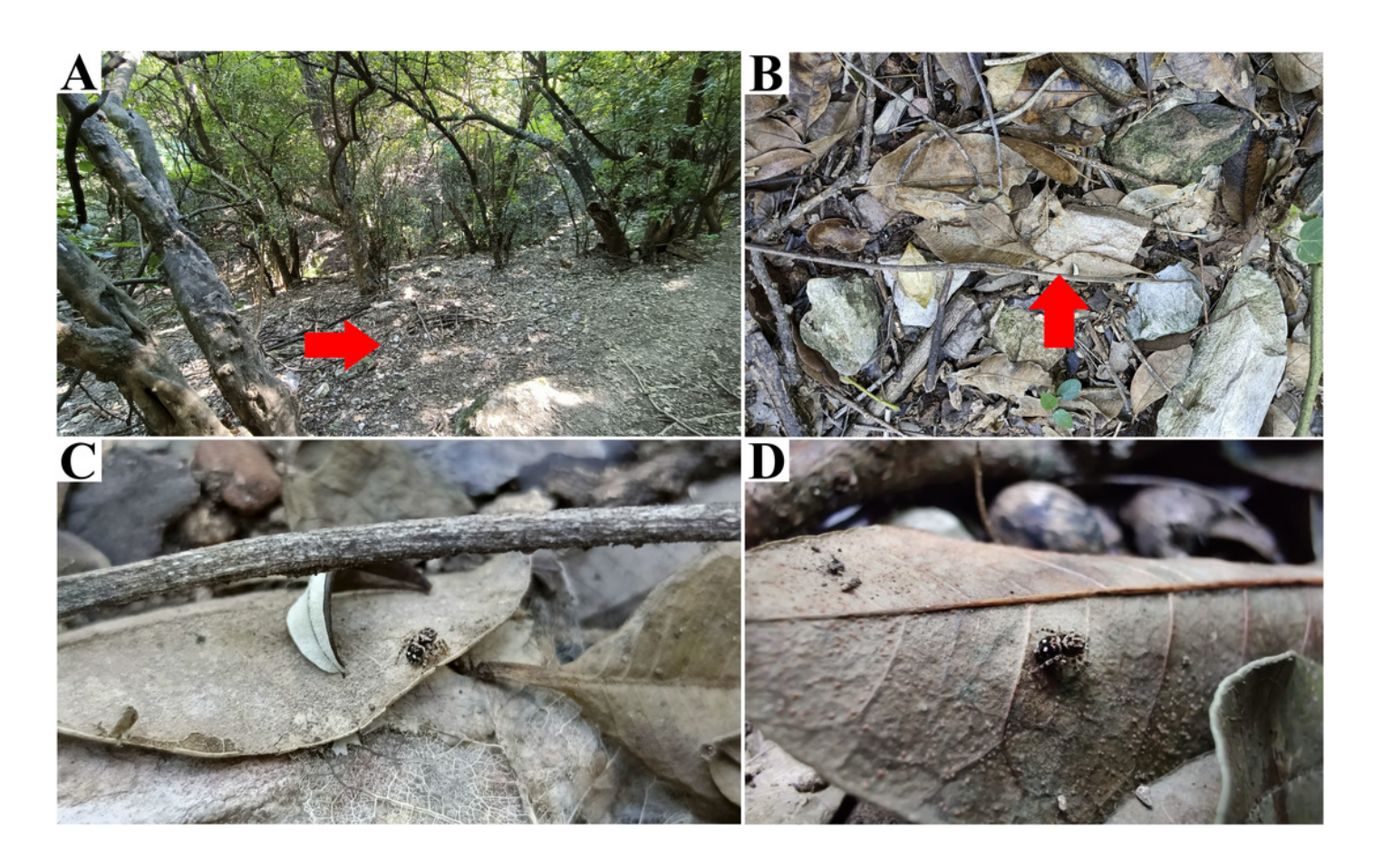
Colors represent putative species. Columns represent the different species delimitation methods. Numbers above branches represent Bootstrap support values for ML (> 50% significant). Column abbreviations: Neighbor-Joining (NJ); General Mixed Yule Coalescent (GMYC); Bayesian Poisson Tree Processes (bPTP) with Maximum Likelihood (ML) and Bayesian Inference (IB) variants; Multi-rate Poisson Tree Processes (mPTP). Red numbers above branches represent Bootstrap support values for ML (> 50% significant).





Naphrys acerba (Peckham & Peckham, 1909) from path to cable car, Cerro de la Silla, Guadalupe, Nuevo León, Mexico.

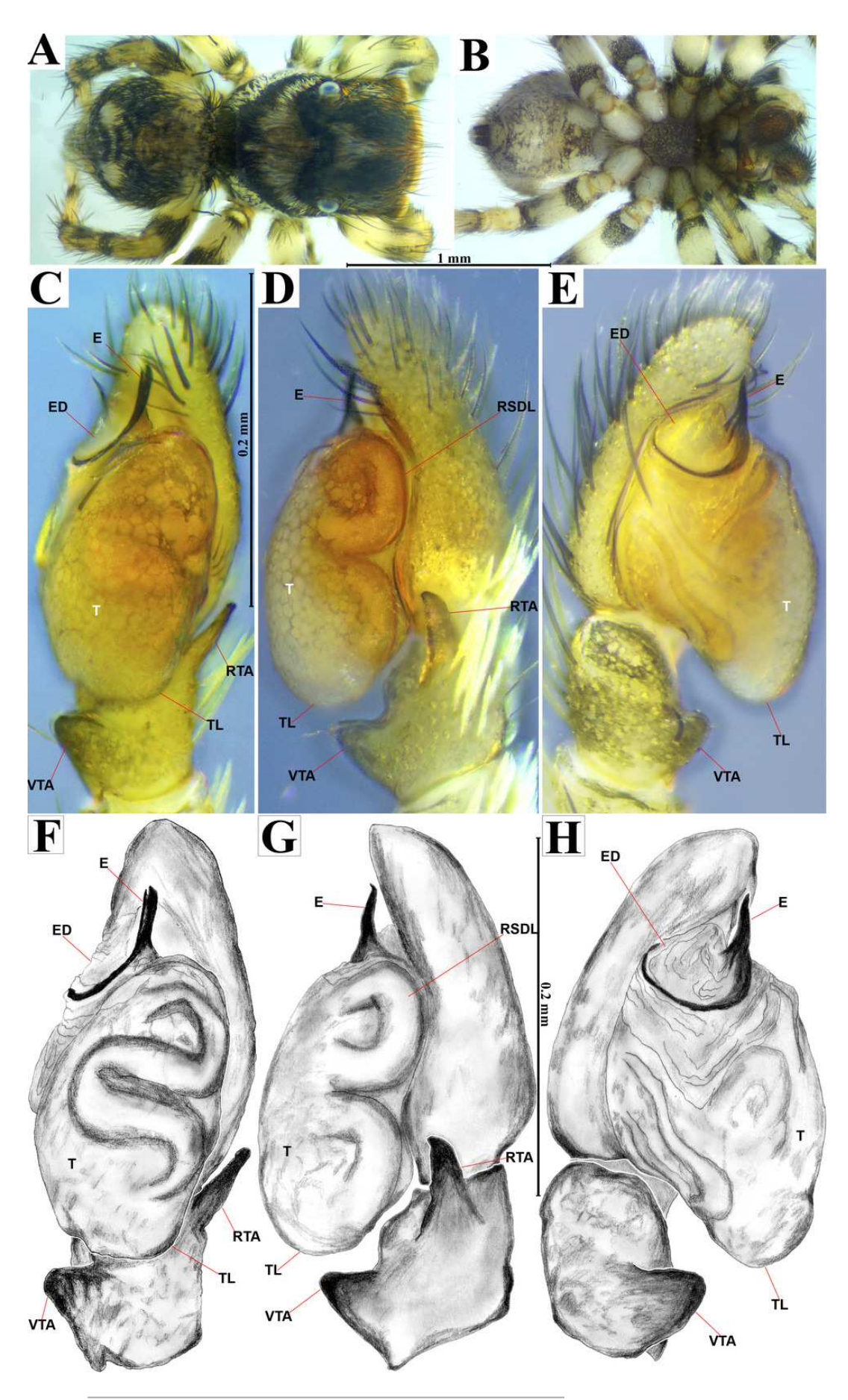
Red arrow indicates A) Habitat, B) Microhabitat. C) and D) Live female on leaf litter. Photos by Juan Maldonado-Carrizales (2023)





Naphrys acerba (Peckham & Peckham, 1909)

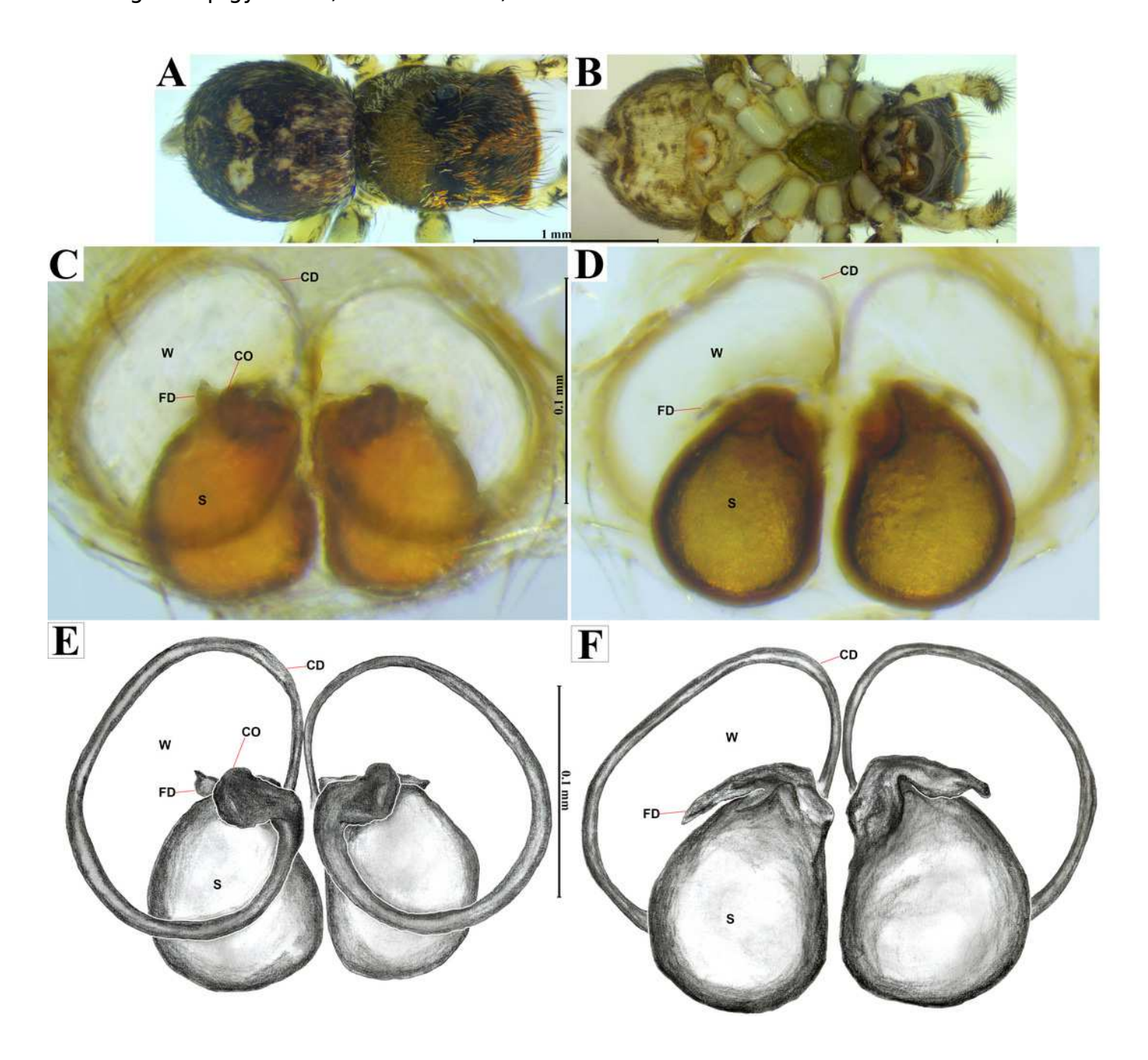
male habitus A) dorsal and B) ventral views. Left palp C) ventral, D) retrolateral and E) prolateral views. Drawings of left palp F) ventral, G) retrolateral and H) prolateral views.



PeerJ reviewing PDF | (2024:07:104276:1:2:CHECK 17 Oct 2024)

Naphrys acerba (Peckham & Peckham, 1909)

female habitus A) dorsal and B) ventral views. Epigynum C) dorsal and D) ventral views. Drawings of epigynum E) ventral and F) dorsal views.



Type locality of *Naphrys echeri* sp. nov. from Cerro El Gigante, Jesús del Monte, Morelia, Michoacán, Mexico.

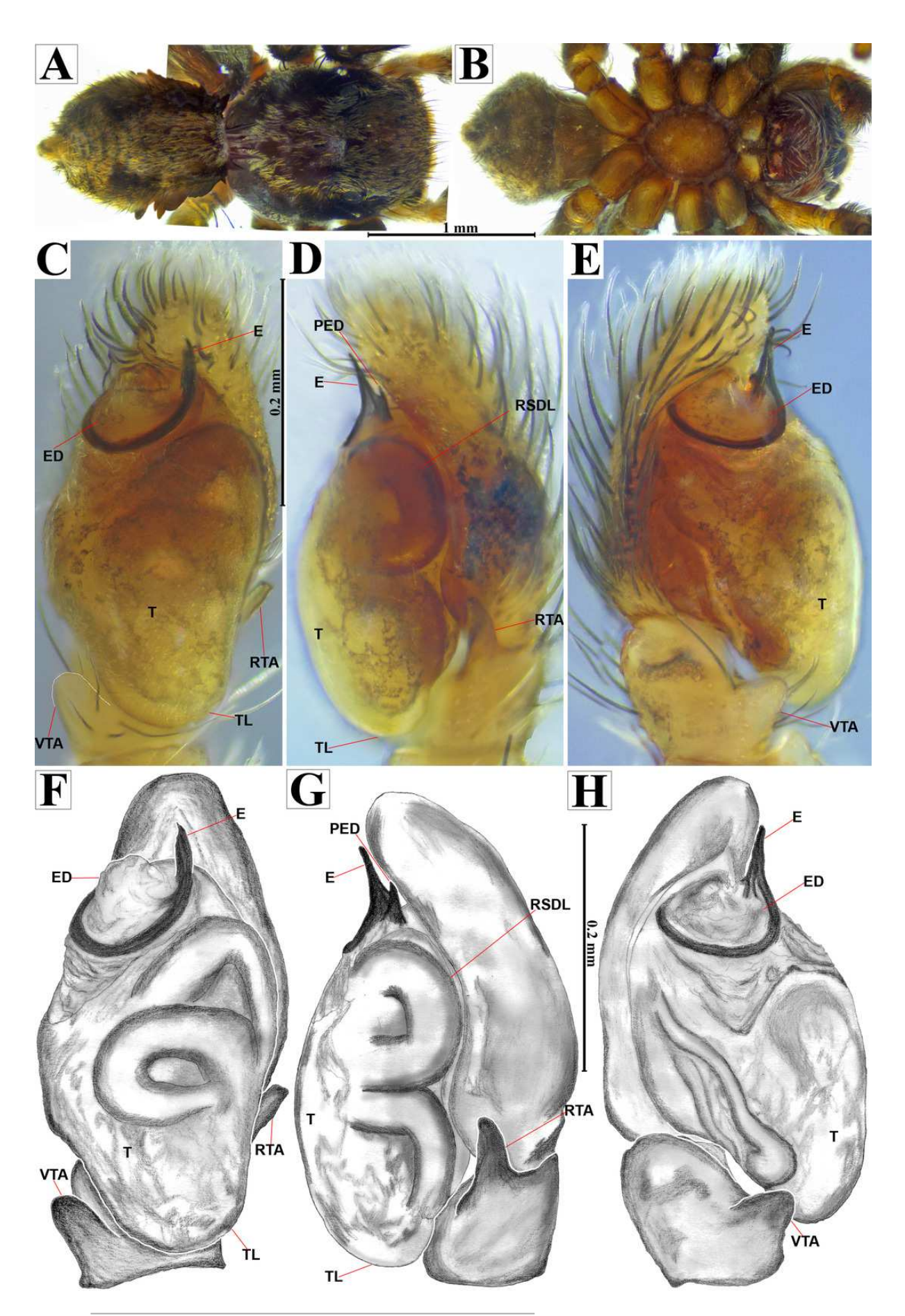
Red arrow indicates A) habitat and B) microhabitat. C) live female specimen in oak forest. Photos by Juan Maldonado-Carrizales (2023).





Naphrys echeri sp. nov. male holotype (CARCIB-AR-047)

habitus A) dorsal and B) ventral views. Left palp C) ventral, D) retrolateral and E) prolateral views. Drawings of left palp F) ventral, G) retrolateral and H) prolateral views.

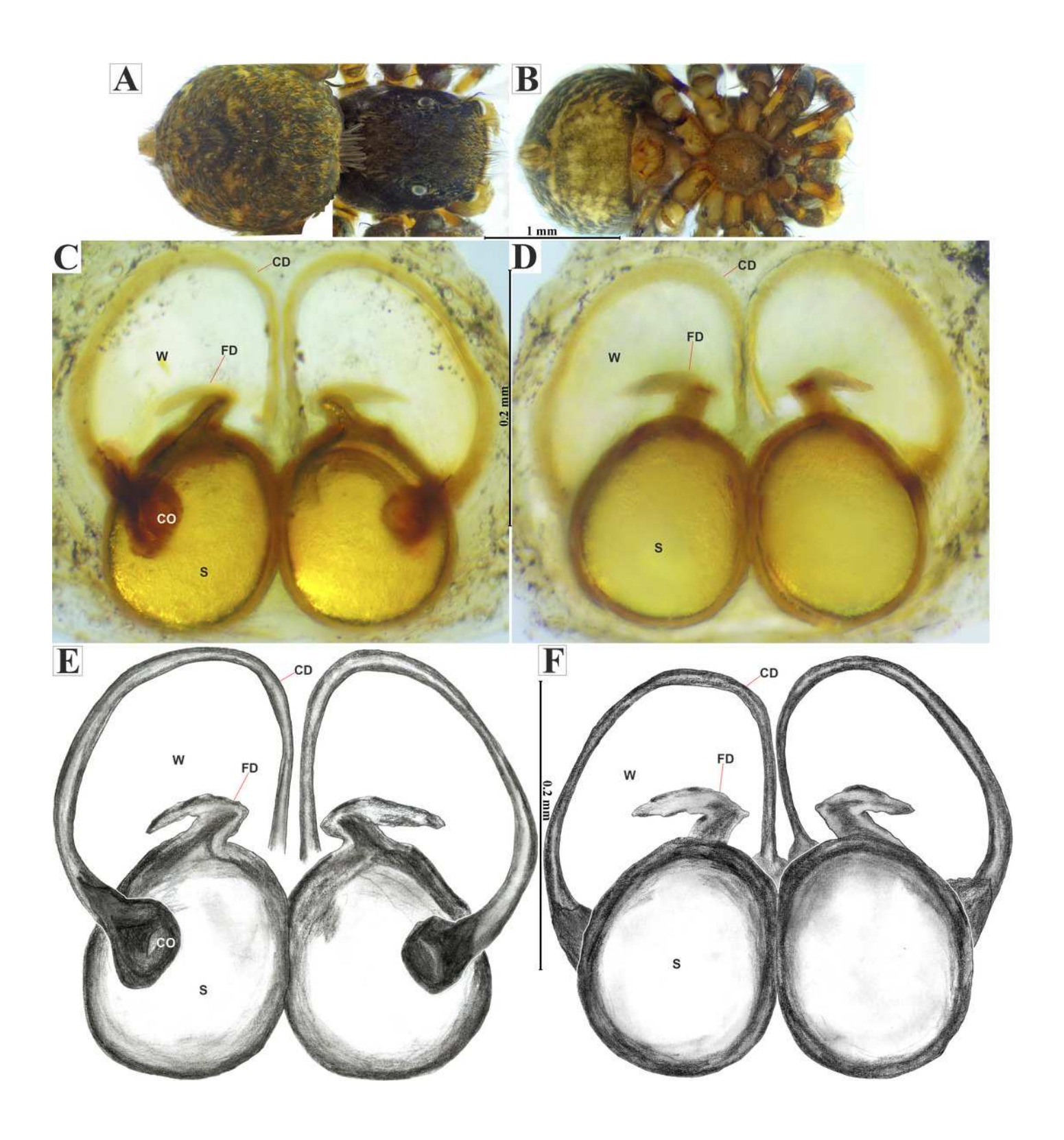


PeerJ reviewing PDF | (2024:07:104276:1:2:CHECK 17 Oct 2024)



Naphrys echeri sp. nov. female allotype (CARCIB-Ar-008)

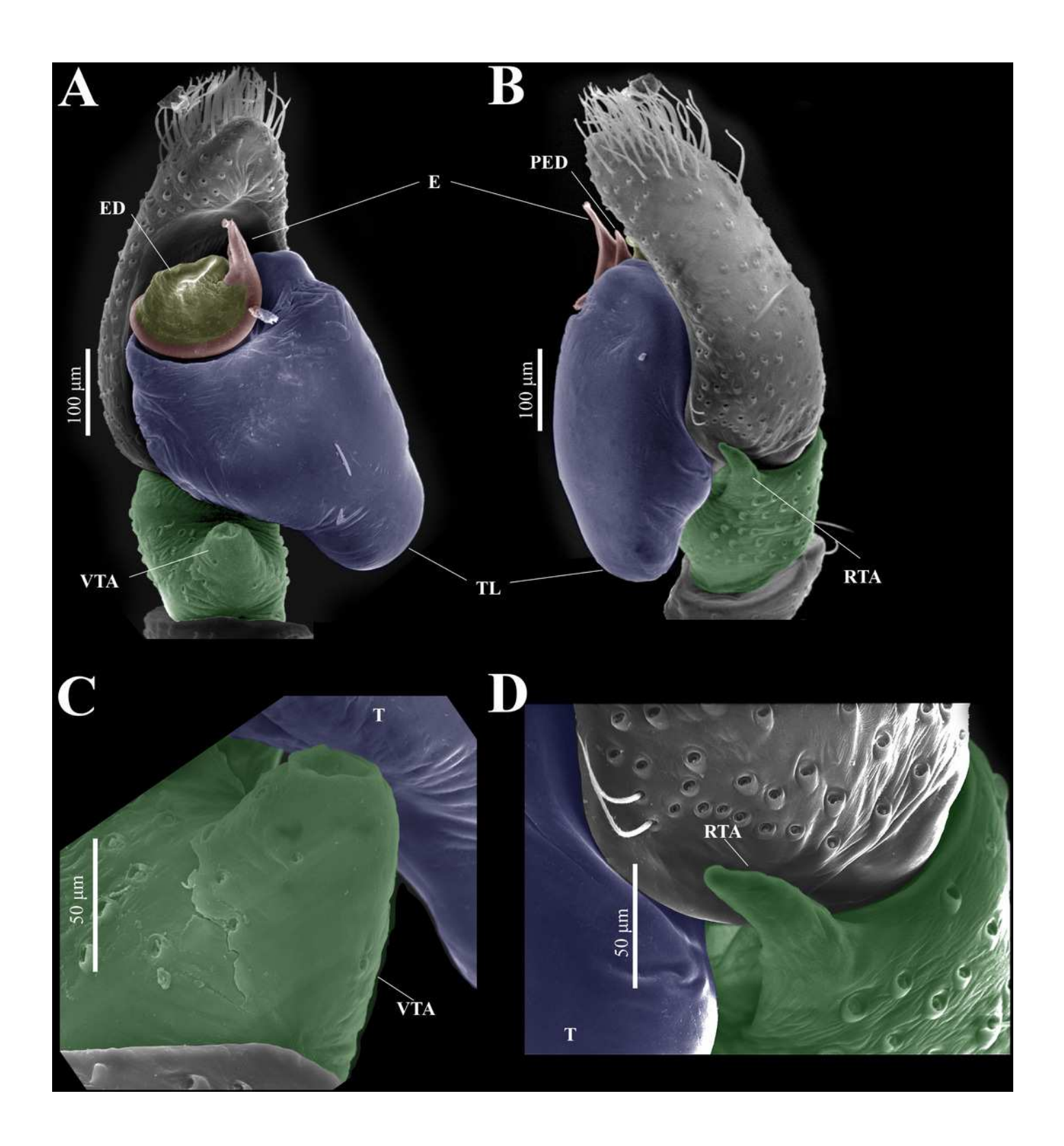
habitus A) dorsal and B) ventral views. epigynum C) dorsal and D) ventral views. Drawings of epigynum E) ventral and F) dorsal views.





Naphrys echeri sp. nov. male genitalia SEM micrographs.

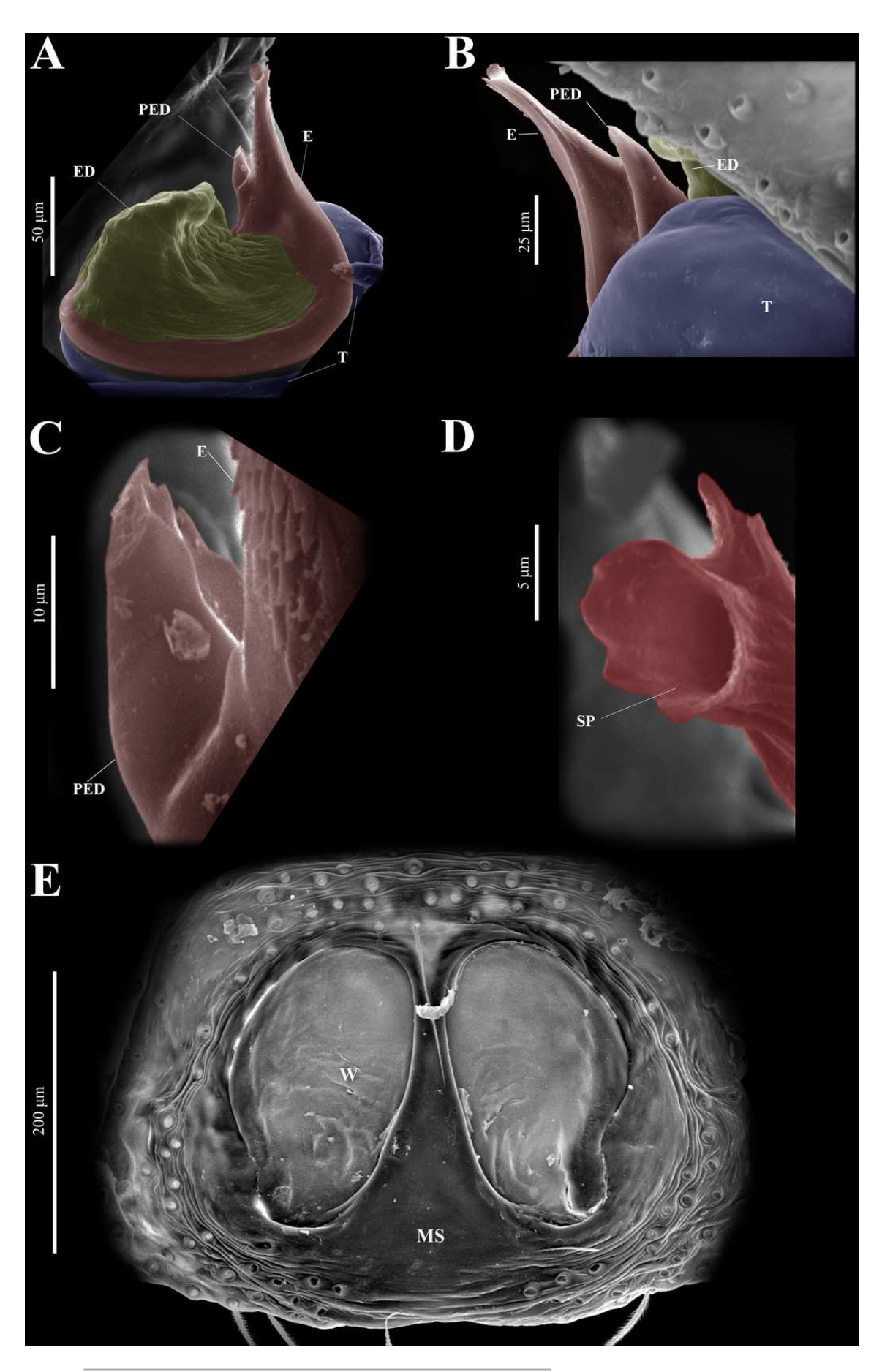
Palp A) prolateral and B) retrolateral views. C) ventral tibial apophysis (VTA). D) retrolateral tibial apophysis (RTA).





Naphrys echeri sp. nov. male genitalia SEM micrographs.

Embolus A) ventral and B) dorsal view. C) process on embolic disc (PED). D) sperm pore (SP) at embolus apex. E) female genitalia SEM micrograph epigynum ventral view.

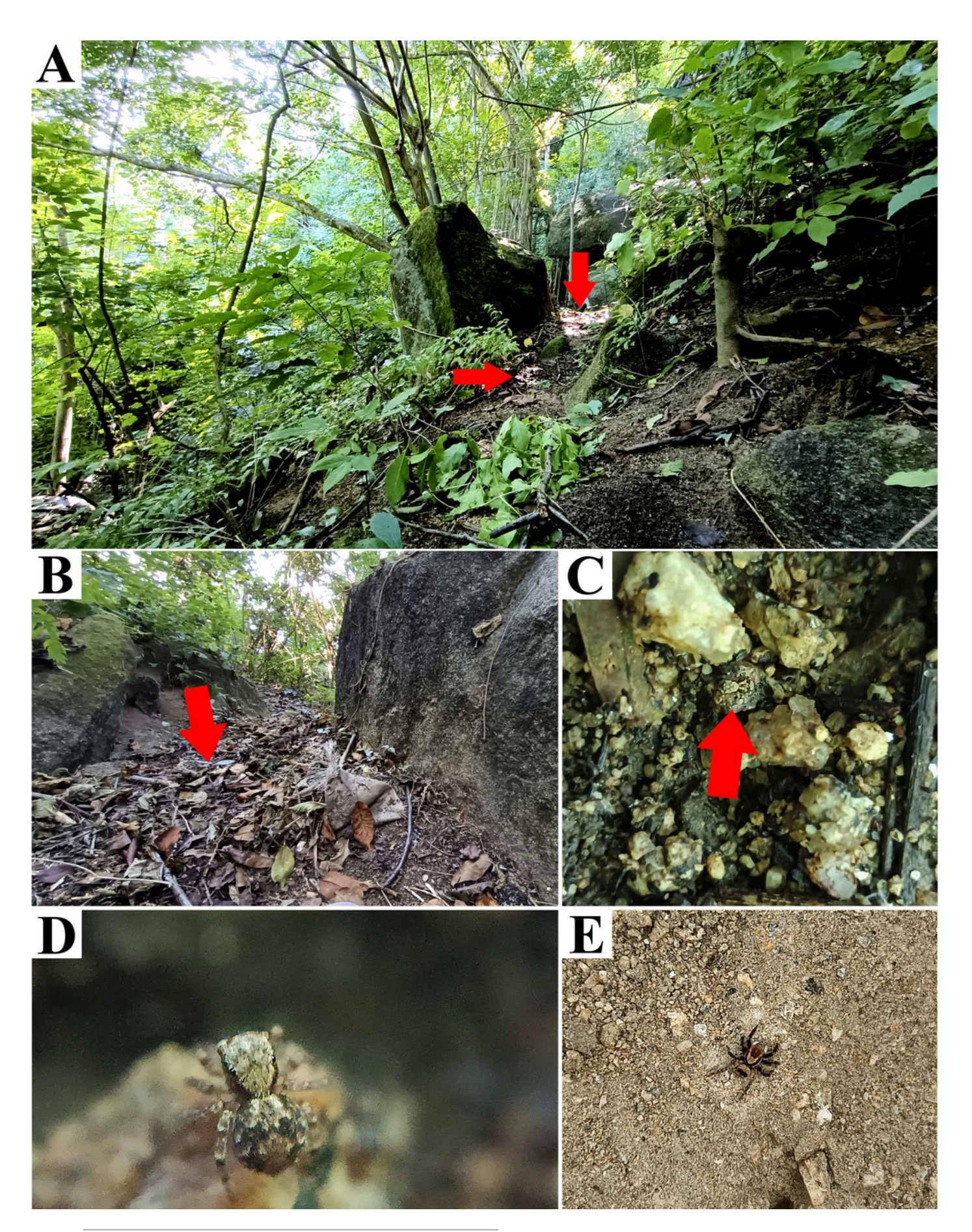


PeerJ reviewing PDF | (2024:07:104276:1:2:CHECK 17 Oct 2024)



Type locality of *Naphrys tecoxquin* sp. nov. from Boca de Tomatlán, Cabo Corrientes, Jalisco, Mexico.

Red arrow indicates A) habitat and B) microhabitat. C) red arrow indicates live specimen on floor. D) female live specimen and E) male live specimen.

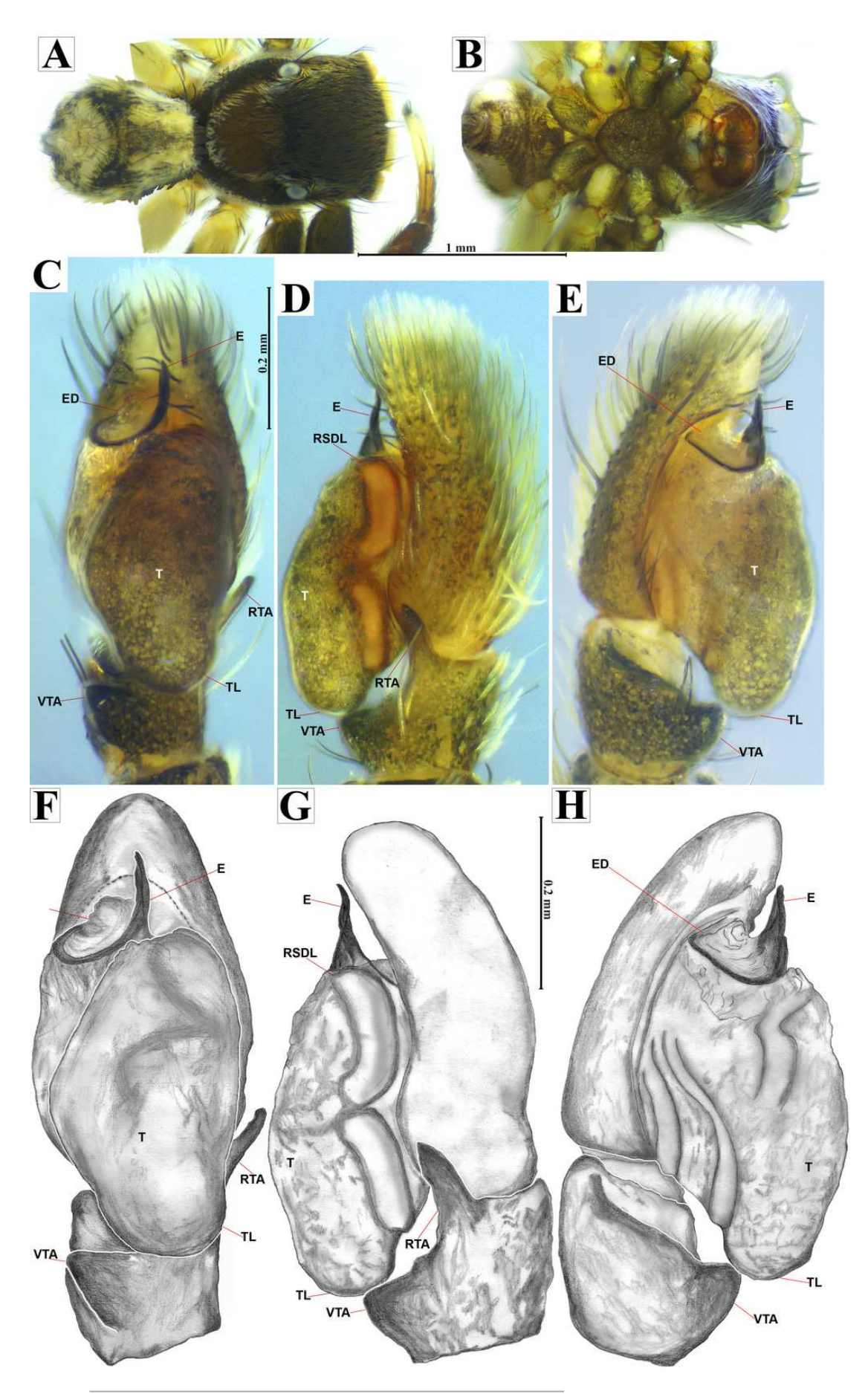


PeerJ reviewing PDF | (2024:07:104276:1:2:CHECK 17 Oct 2024)



Naphrys tecoxquin sp. nov. male holotype (CARCIB-Ar-048)

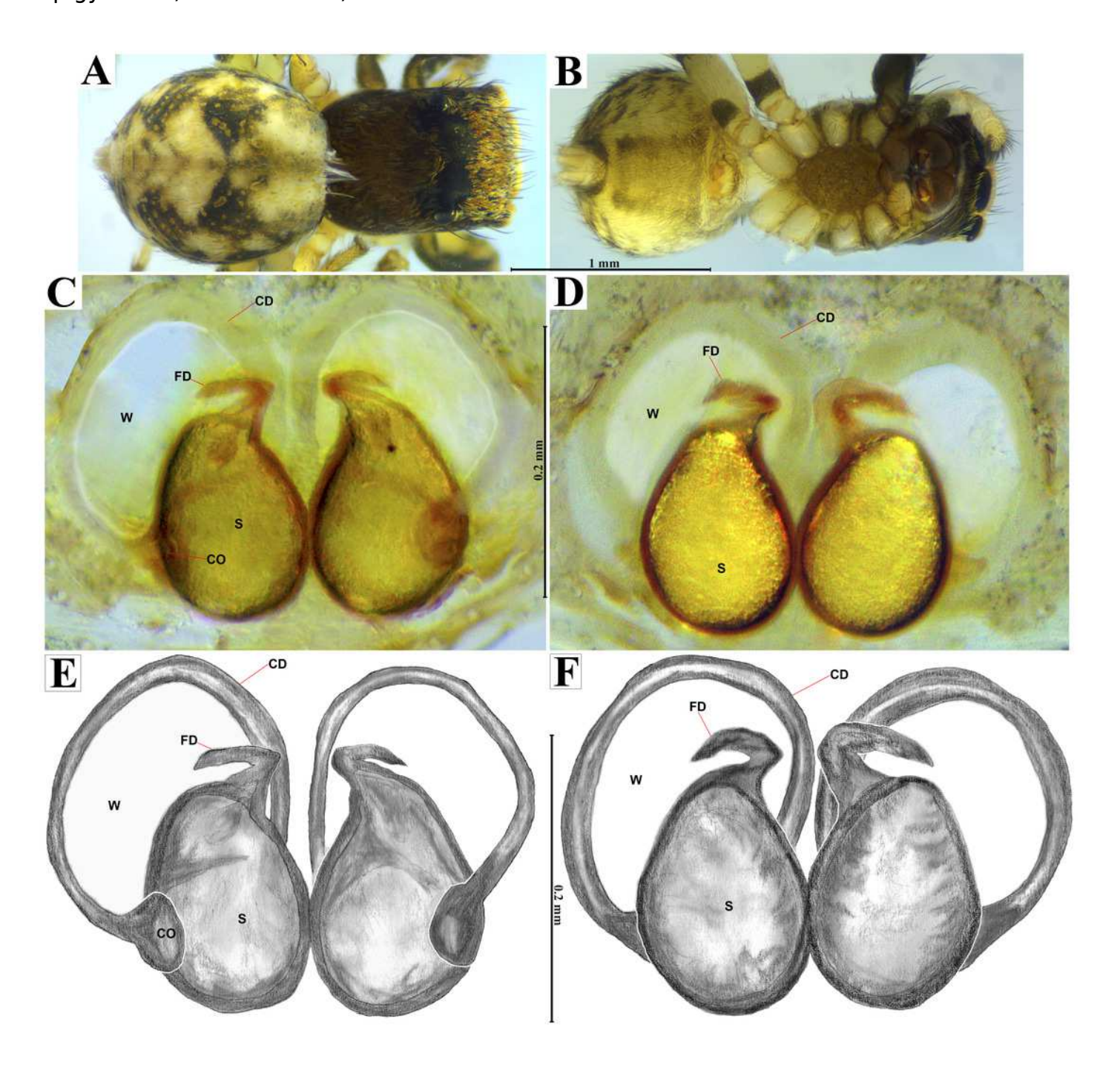
habitus A) dorsal and B) ventral views. Left palp C) ventral, D) retrolateral and E) prolateral views. Drawings of left palp F) ventral, G) retrolateral and H) prolateral views.



PeerJ reviewing PDF | (2024:07:104276:1:2:CHECK 17 Oct 2024)

Naphrys tecoxquin sp. nov. female allotype (CARCIB-Ar-009)

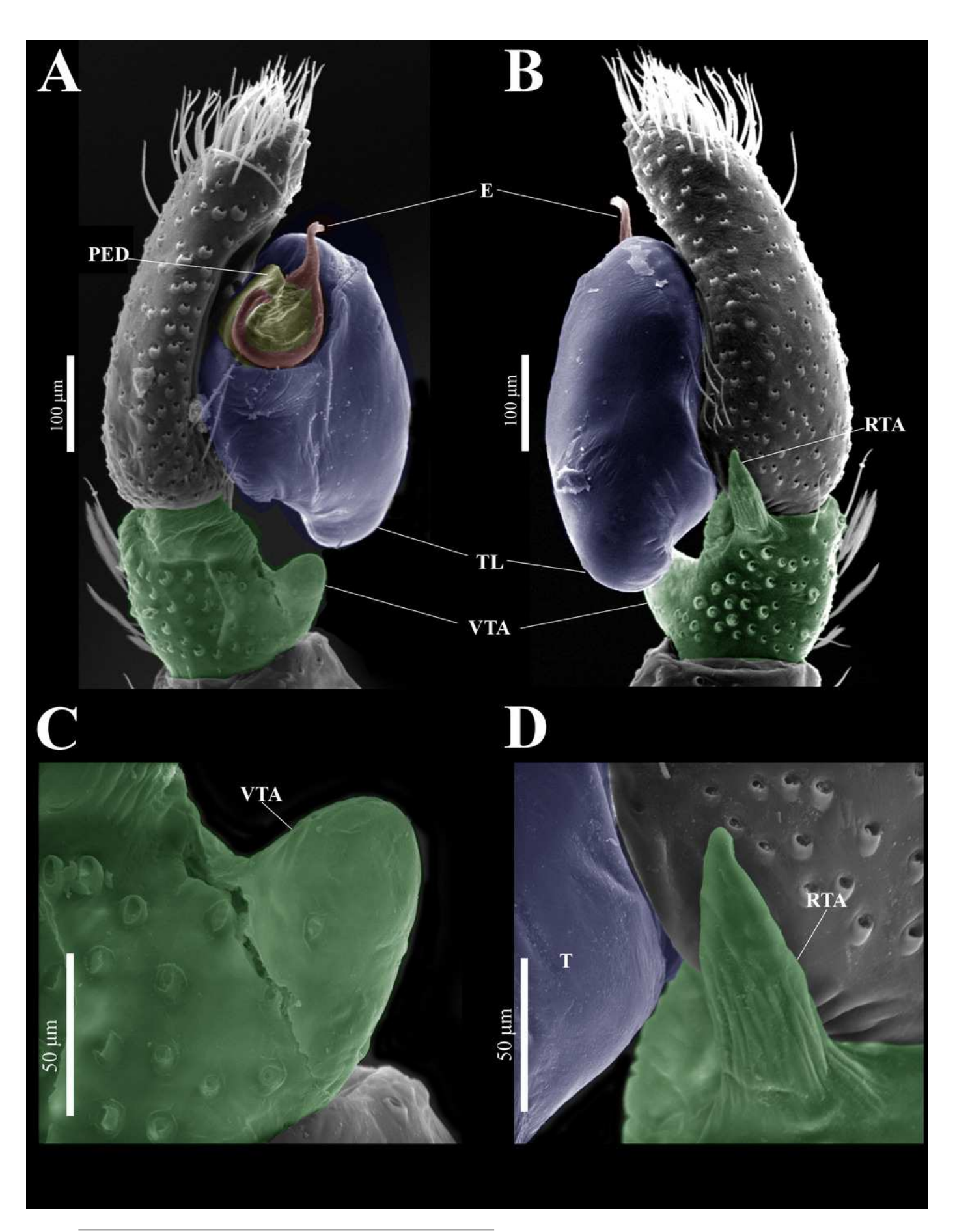
habitus A) dorsal and B) ventral views. epigynum C) dorsal and D) ventral views. Drawings of epigynum E) ventral and F) dorsal views.





Naphrys tecoxquin sp. nov. male genitalia SEM micrographs.

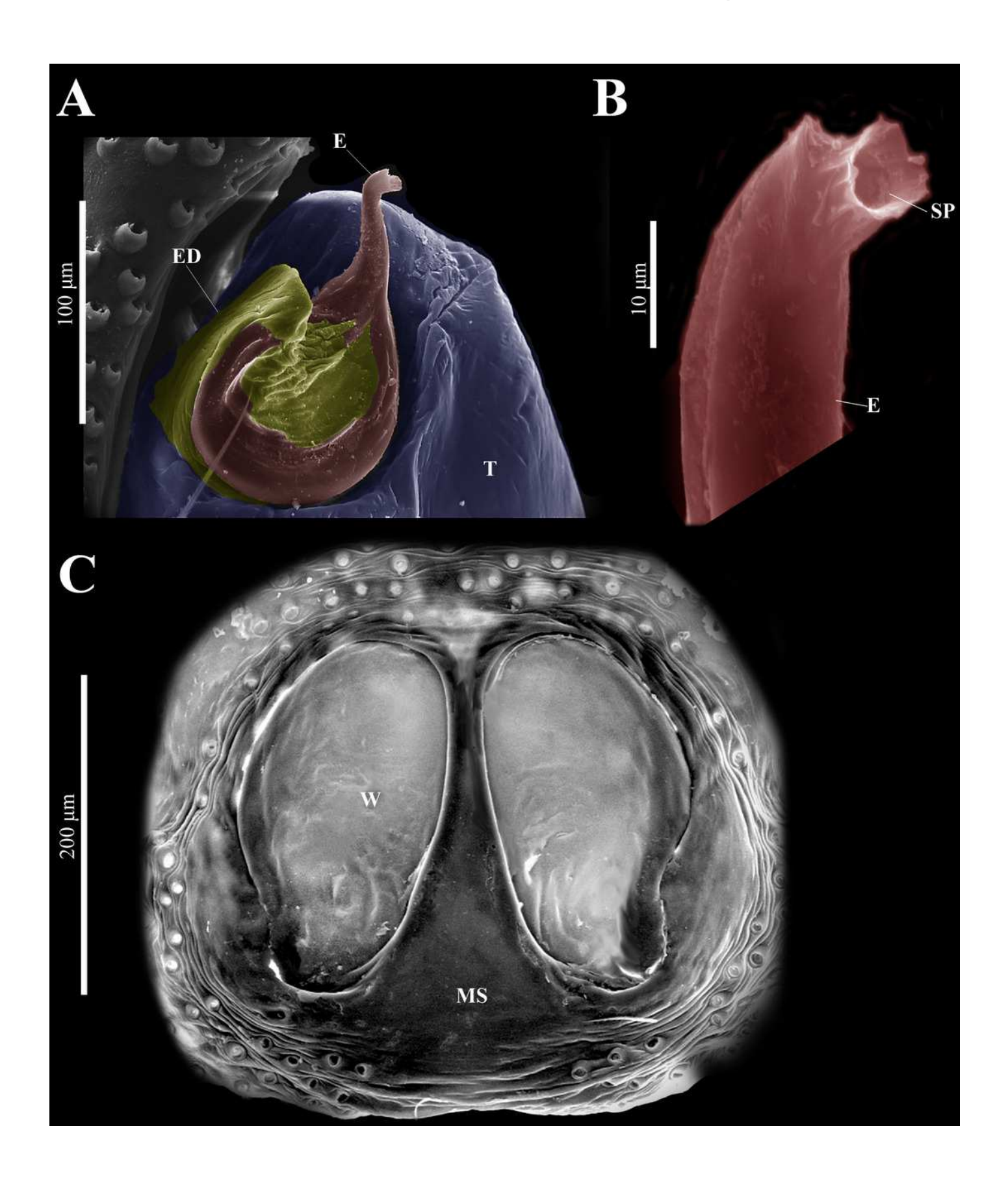
Palp A) prolateral and B) retrolateral views. C) ventral tibial apophysis (VTA). D) retrolateral tibial apophysis (RTA).





Naphrys tecoxquin sp. nov. male genitalia SEM micrographs.

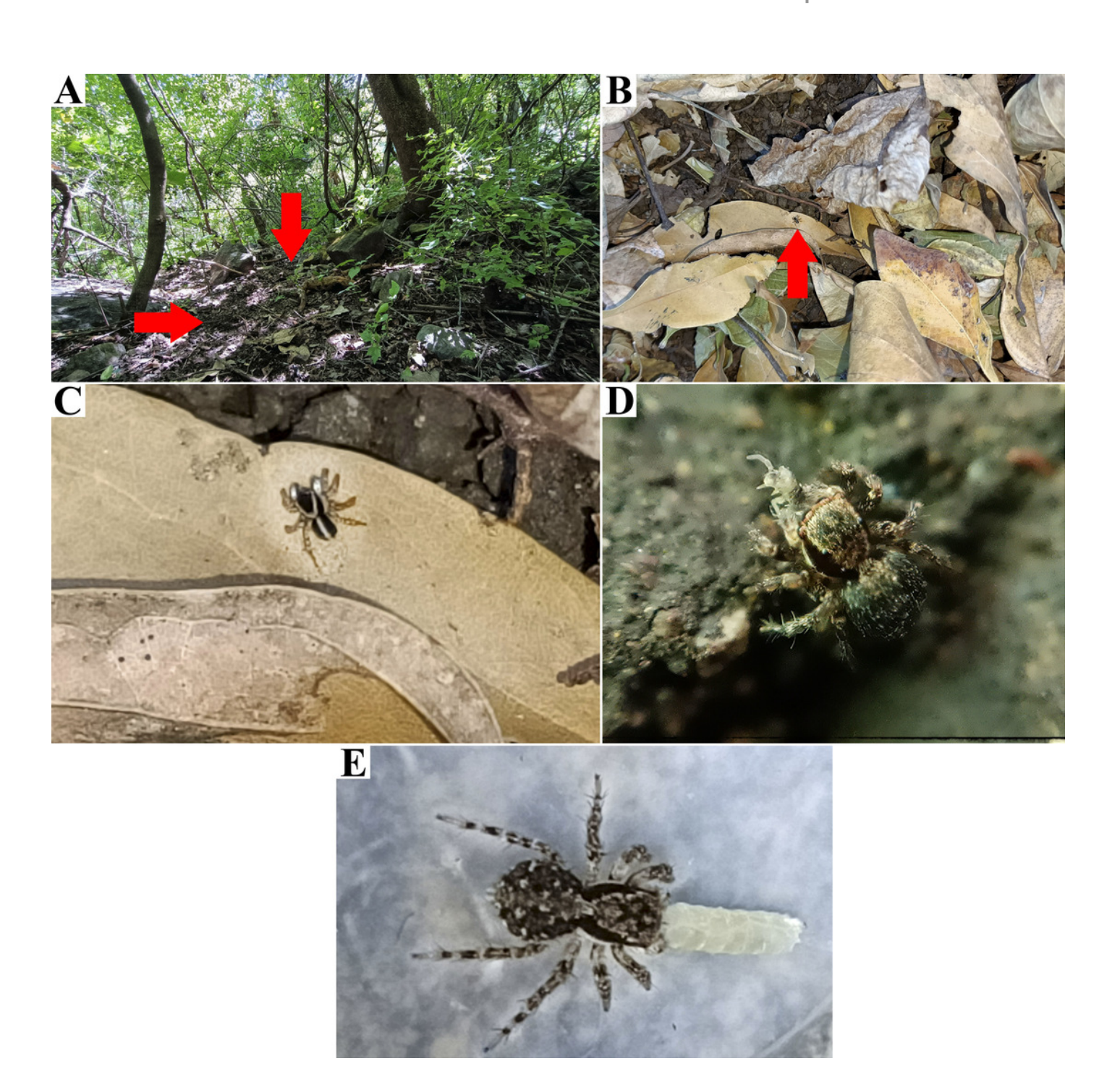
Embolus A) ventral view. B) sperm pore (SP) at embolus apex. C) female genitalia SEM micrograph epigynum ventral view.





Type locality of Naphrys tuuca sp. nov. from Cerro San Juan, Tepic, Nayarit, Mexico.

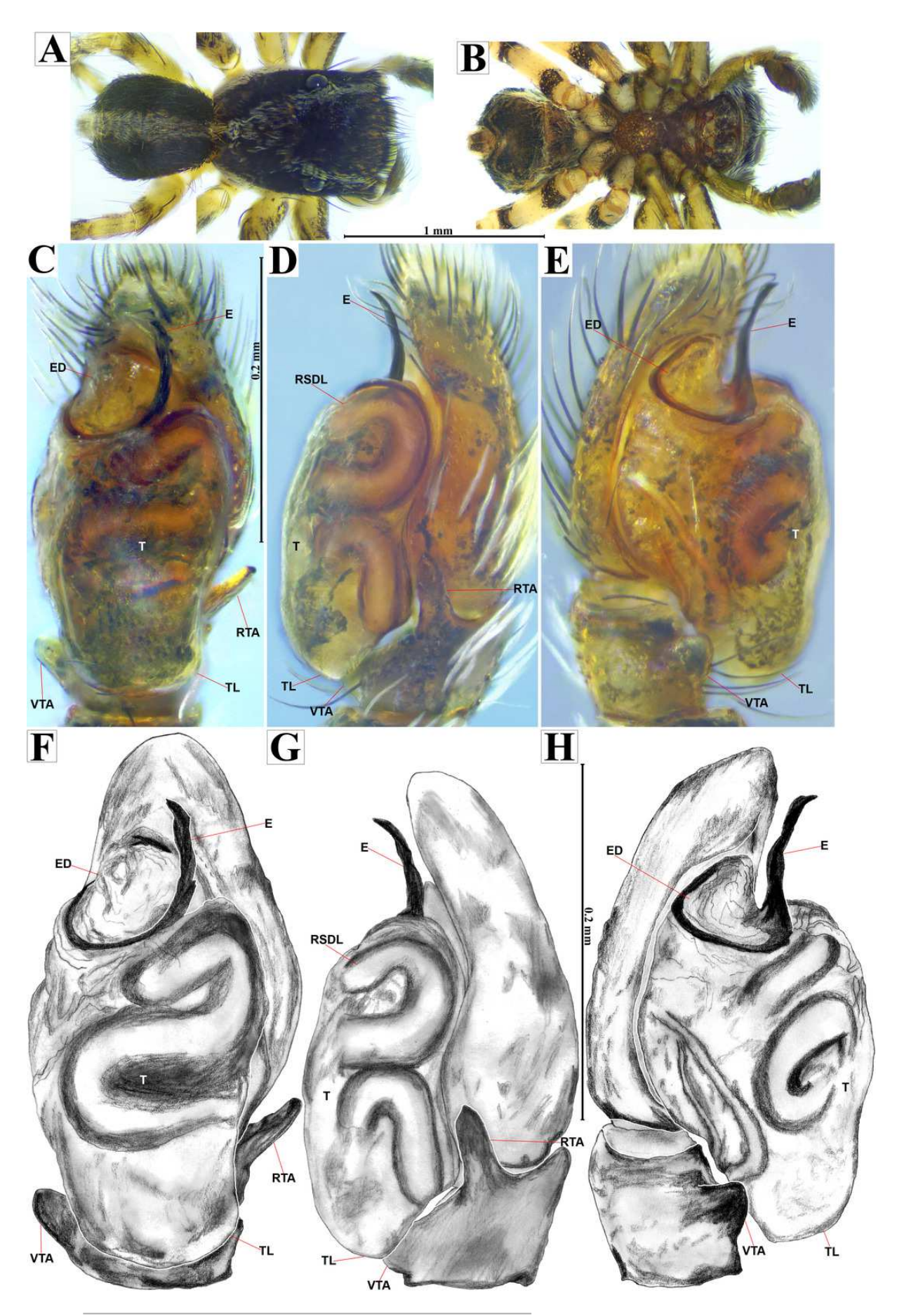
Red arrow indicates A) habitat and B) microhabitat. C) live male specimen. D) live female eating a Collembola in field. E) live female eating a larva of *Drosophila melanogaster* Meigen, 1830 in captivity. Photos by Juan Maldonado-Carrizales (2023).





Naphrys tuuca sp. nov. male holotype (CARCIB-Ar-049)

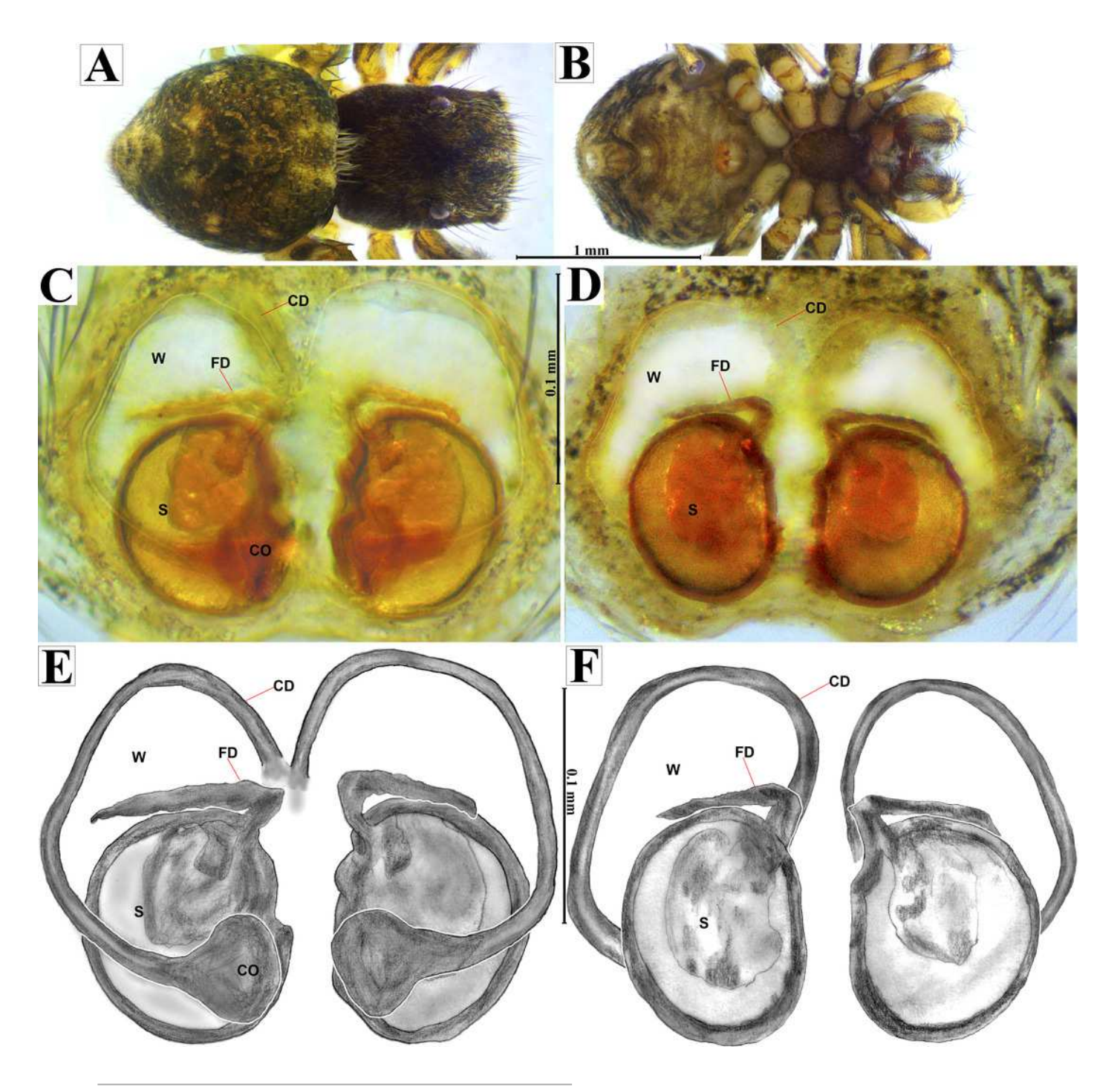
habitus A) dorsal and B) ventral views. Left palp C) ventral, D) retrolateral and E) prolateral views. Drawings of left palp F) ventral, G) retrolateral and H) prolateral views.



PeerJ reviewing PDF | (2024:07:104276:1:2:CHECK 17 Oct 2024)

Naphrys tuuca sp. nov. female allotype (CARCIB-Ar-010)

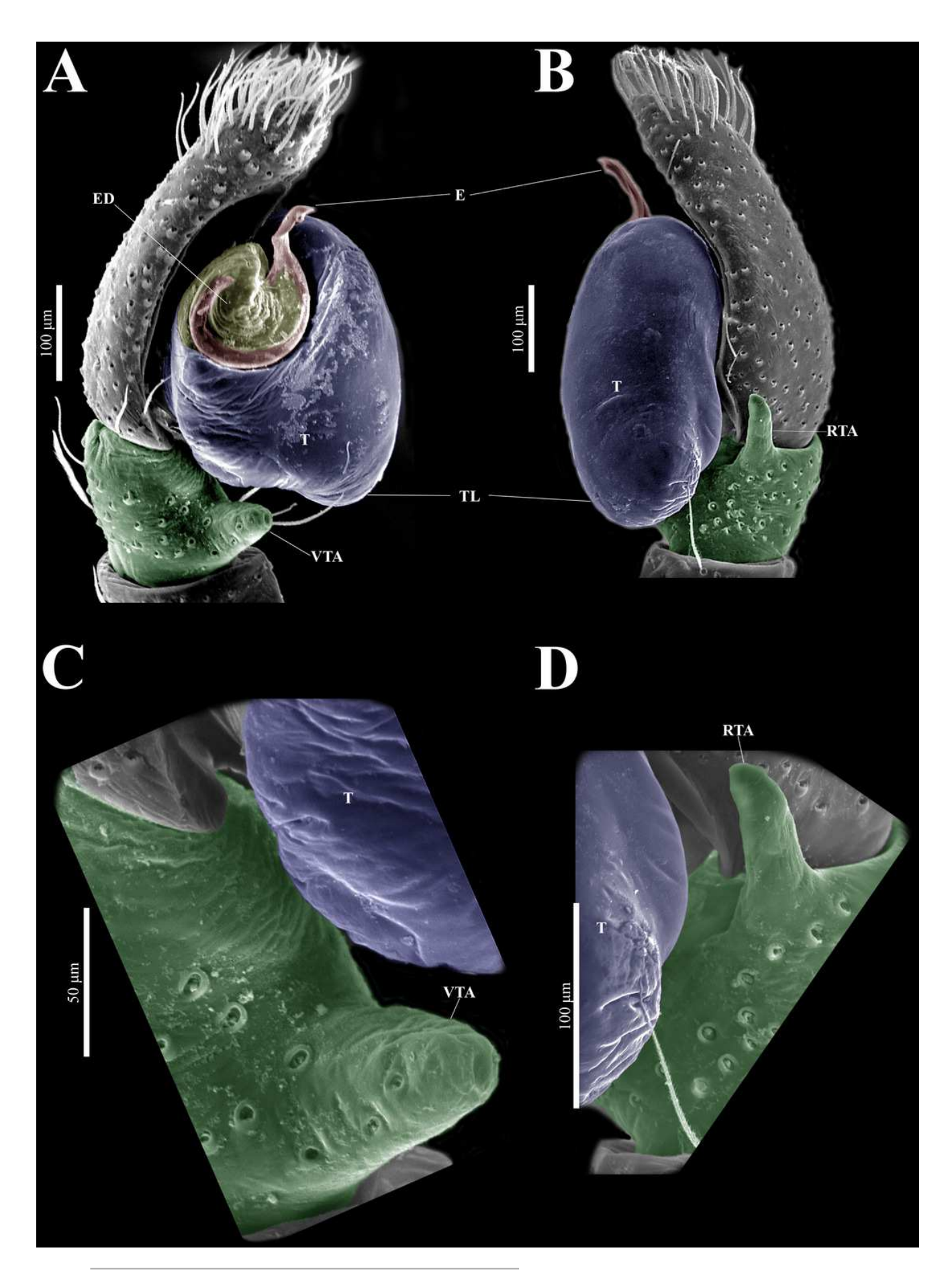
habitus A) dorsal and B) ventral views. epigynum C) dorsal and D) ventral views. Drawings of epigynum E) ventral and F) dorsal views.





Naphrys tuuca sp. nov. male genitalia SEM micrographs.

Palp A) prolateral and B) retrolateral views. C) ventral tibial apophysis (VTA). D) retrolateral tibial apophysis (RTA).

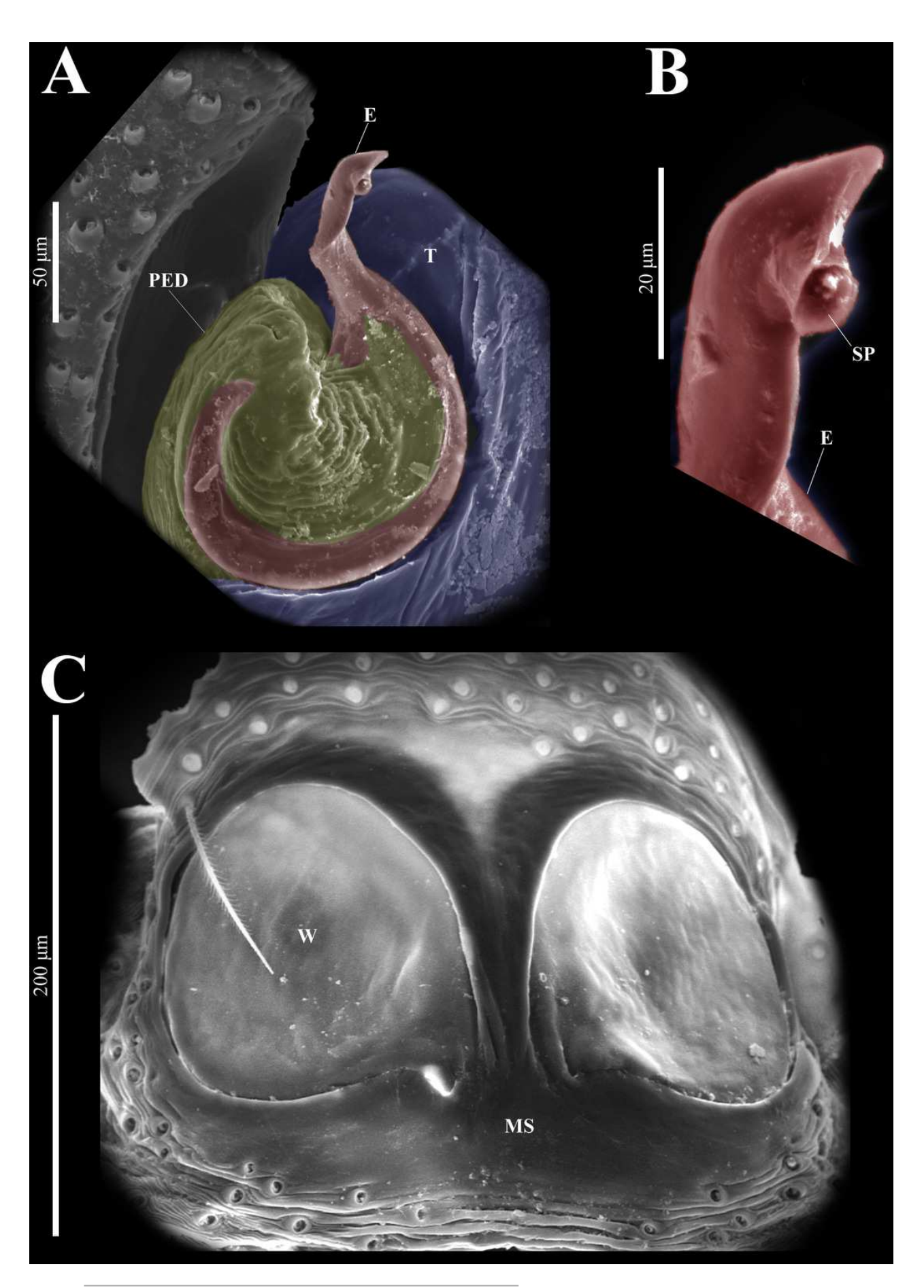


PeerJ reviewing PDF | (2024:07:104276:1:2:CHECK 17 Oct 2024)



Naphrys tuuca sp. nov. male genitalia SEM micrographs.

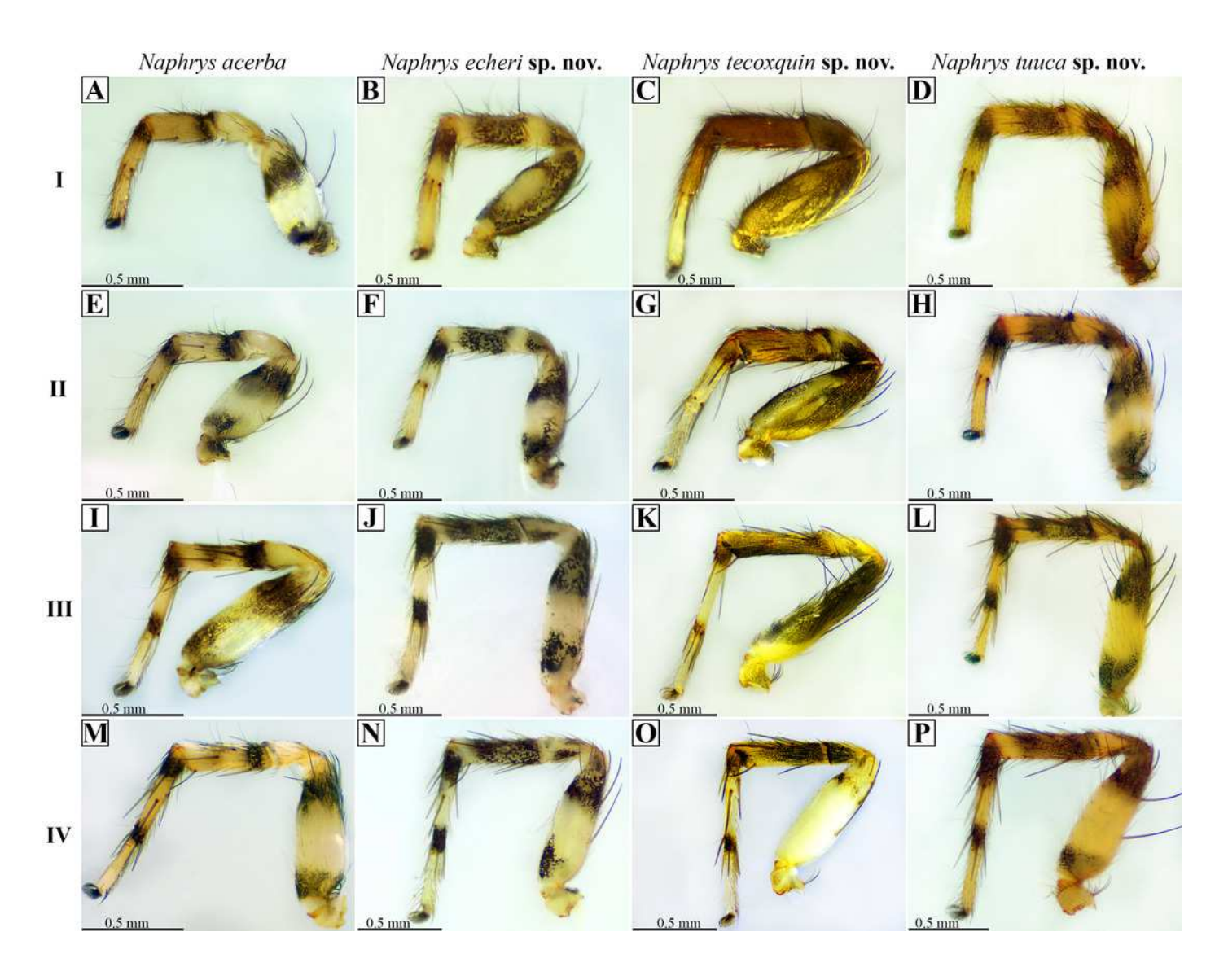
Embolus A) ventral view. B) sperm pore (SP) at embolus apex. C) female genitalia SEM micrograph epigynum ventral view.



PeerJ reviewing PDF | (2024:07:104276:1:2:CHECK 17 Oct 2024)

Retrolateral view of male Naphrys legs.

Left column indicates leg number. Top row indicates species. A), E), I) & M) legs I, II, III & IV of Naphrys acerba, respectively; B), F), J) & N) legs I, II, III, IV of Naphrys echeri sp. nov., respectively; C), G), K) & O) legs I, II, III, IV of Naphrys tecoxquin sp. nov., respectively; D), H), L) & P) legs I, II, III, IV of Naphrys tuuca sp. nov., respectively.



Known distribution records of the Mexican species of Naphrys.

Star: *N. acerba*. Diamond: *N. echeri* sp. nov.. Circle: *N. tecoxquin* sp. nov. Cross: *N. tuuca* sp. nov. Colors represent the biogeographical provinces following Escalante, Rodríguez-Tapia & Morrone (2021). Blue: Transmexican Volcanic Belt province. Green: Sierra Madre del Sur Province. Pink: Sierra Madre Oriental. Yellow: Pacific Lowlands.

